

Accepted Manuscript

Incorporation of histone deacetylase inhibitory activity into the core of tamoxifen - a new hybrid design paradigm

Anthony F. Palermo, Marine Diennet, Mohamed El Ezzy, Benjamin M. Williams, David Cotnoir-White, Sylvie Mader, James L. Gleason

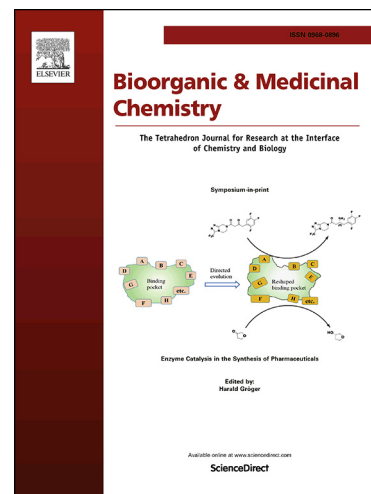
PII: S0968-0896(18)30433-4
DOI: <https://doi.org/10.1016/j.bmc.2018.07.026>
Reference: BMC 14463

To appear in: *Bioorganic & Medicinal Chemistry*

Received Date: 23 March 2018
Revised Date: 5 July 2018
Accepted Date: 14 July 2018

Please cite this article as: Palermo, A.F., Diennet, M., El Ezzy, M., Williams, B.M., Cotnoir-White, D., Mader, S., Gleason, J.L., Incorporation of histone deacetylase inhibitory activity into the core of tamoxifen - a new hybrid design paradigm, *Bioorganic & Medicinal Chemistry* (2018), doi: <https://doi.org/10.1016/j.bmc.2018.07.026>

This is a PDF file of an unedited manuscript that has been accepted for publication. As a service to our customers we are providing this early version of the manuscript. The manuscript will undergo copyediting, typesetting, and review of the resulting proof before it is published in its final form. Please note that during the production process errors may be discovered which could affect the content, and all legal disclaimers that apply to the journal pertain.



Graphical Abstract

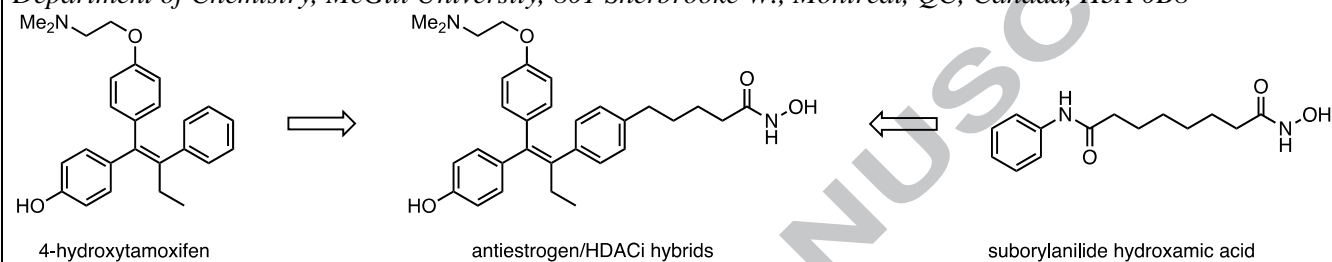
To create your abstract, type over the instructions in the template box below.
 Fonts or abstract dimensions should not be changed or altered.

Incorporation of histone deacetylase inhibitory activity into the core of tamoxifen - a new hybrid design paradigm

Leave this area blank for abstract info.

Anthony F. Palermo, Marine Diennet, Mohamed El Ezzy, Benjamin M. Williams, David Cotnoir-White, Sylvie Mader* and James L. Gleason*

Department of Chemistry, McGill University, 801 Sherbrooke W., Montreal, QC, Canada, H3A 0B8





Incorporation of histone deacetylase inhibitory activity into the core of tamoxifen - a new hybrid design paradigm.

Anthony F. Palermo,^{1,5} Marine Diennet,^{2,5} Mohamed El Ezzy,² Benjamin M. Williams,¹ David Cotnoir-White,² Sylvie Mader^{*,2,3,4} and James L. Gleason^{*,1}

¹ Department of Chemistry, McGill University, 801 Sherbrooke W., Montreal, QC, Canada, H3A 0B8

² Institute for Research in Immunology and Cancer, Pavillon Marcelle-Coutu, Université de Montréal, 2950 chemin de Polytechnique, Montréal, QC, Canada, H3T 1J4

³ Biochemistry Department, Pavillon Roger-Gaudry, Université de Montréal, 2900 Bd Edouard Montpetit, Montréal, QC, Canada, H3T 1J4

⁴ Centre de Recherche du CHUM, Université de Montréal, Montréal, QC, Canada, H2X 0A9

⁵ These authors contributed equally to this manuscript.

ARTICLE INFO

Article history:

Received

Received in revised form

Accepted

Available online

Keywords:

Keyword_1

Keyword_2

Keyword_3

Keyword_4

Keyword_5

ABSTRACT

Hybrid antiestrogen / histone deacetylase (HDAC) inhibitors were designed by appending zinc binding groups to the 4-hydroxystilbene core of 4-hydroxytamoxifen. The resulting hybrids were fully bifunctional, and displayed high nanomolar to low micromolar IC₅₀ values against both the estrogen receptor α (ER α) and HDACs *in vitro* and in cell-based assays. The hybrids were antiproliferative against ER+ MCF-7 breast cancer cells, with hybrid **28b** possessing an improved activity profile compared to either 4-hydroxytamoxifen or SAHA. Hybrid **28b** displayed gene expression patterns that reflected both ER α and HDAC inhibition.

2009 Elsevier Ltd. All rights reserved.

1. Introduction

Estrogens, mainly 17 β -estradiol (E2, **1**, Fig 1), are the primary hormones responsible for the development of female secondary sexual characteristics, including normal growth of the mammary gland.¹ E2 genomic signalling occurs mainly through estrogen receptor- α and - β (ER α and ER β), members of the nuclear receptor superfamily of ligand-activated transcription factors.² Binding of E2 to ERs results in a conformational change that involves the folding of helix 12 (H12) over the ligand binding pocket (LBP), which induces receptor binding to DNA at estrogen response elements (EREs) located in the regulatory regions of target genes, release of transcriptional co-repressors, and the recruitment of co-activators and transcription machinery.

Expression of ER α , which is observed in about 70% of breast tumors, mediates the growth-stimulatory effects of estrogens on these tumors.³⁻⁵ Efforts to inhibit E2-mediated tumor growth have led to the development of ER antagonists as therapeutic tools for ER+ breast cancer. The most commonly employed antiestrogen (AE) has been tamoxifen (**2**), which is classified as a selective estrogen receptor modulator (SERM) for its tissue-specific

effects on estrogen signaling. In breast, it antagonizes estrogen-induced growth, while it has agonist activity for expression of estrogen target genes in uterine cells.⁶⁻⁹ Tamoxifen itself has low affinity for ERs and acts mainly as a prodrug. It is oxidized *in vivo* to several active metabolites, including 4-hydroxytamoxifen (4-OHT, **3**) and endoxifen, which have potent antiproliferative activities in ER+ breast cancer cells *in vitro*.^{10, 11} Tamoxifen is used in first line endocrine therapy of all stages of ER+ breast tumors, especially in pre-menopausal women as aromatase inhibitors have demonstrated superior efficacy in the post-menopausal setting.¹² Tamoxifen has an overall clinical response rate of about 50%, although it is less effective in metastatic cases.^{12,13,12, 14} Unfortunately, relapse in patients with primary tumors can occur years after treatment, suggesting incomplete eradication of tumor cells and benefit from extension of hormonal therapy to 10 years instead of five.¹⁵ A second class of antiestrogens called pure antiestrogens or selective estrogen receptor down-regulators (SERDs) are devoid of the partial agonist activity of tamoxifen in the uterus and possess the ability to induce SUMOylation, ubiquitination, and degradation of ER α .¹⁶⁻¹⁸ The SERD fulvestrant (**5**) has proven beneficial as a

second line therapy for patients that have previously undergone hormonal treatment.^{19, 20}

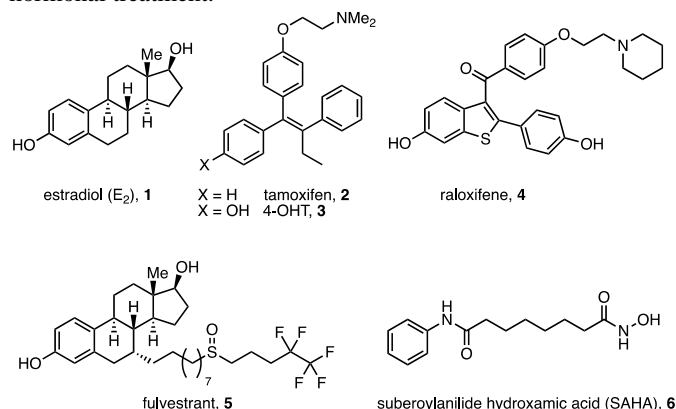


Figure 1. Structures of antiestrogens and HDAC inhibitors.

Histone deacetylases (HDACs) function as transcriptional co-regulators, modulating in combination with histone acetyl transferases the acetylation state of histones and the accessibility of DNA in chromatin.²¹ In addition, HDACs are also known to deacetylate non-genomic targets such as tubulin, HSP90, and p53.²² HDACs are overexpressed in many cancers, including breast cancer.^{23, 24} Several HDAC inhibitors (HDACi's) are clinically approved for blood cancer indications and have been investigated in combination with other agents for use in solid tumors, including breast cancer.^{25,26,27} The prototype of this class is suberoylanilide hydroxamic acid (SAHA, **6**, Fig 1), which has been approved for treatment of cutaneous T-cell lymphoma.²⁸

Several studies have shown a combinatorial effect of HDACi's and antiestrogens in breast cancer. Tamoxifen exhibited cooperativity with several HDACi's to inhibit growth of ER+ MCF-7 breast cancer *in vitro* and *in vivo*.^{29, 30} Other studies have shown combinatorial effects of antiestrogens and HDACi's in both ER+ and ER- breast cancer cell lines.³¹⁻³³ Moreover, the combination of tamoxifen and SAHA was shown in a phase II study to have a 40% clinical benefit for patients with ER+ tumors that had progressed during endocrine therapy.³⁴

Based on the synergy between antiestrogens and HDACi's, several groups including ours have investigated hybrid structures that combine both biochemical activities in a single molecule.³⁵⁻³⁹ Our previous work incorporated HDACi function in the side-chain of fulvestrant (**7**, Fig 2).³⁵ Other hybrids have also incorporated HDACi function in the side-chains of raloxifene (**8**) and tamoxifen (**9**).³⁷⁻³⁹ While all these hybrids possessed antiproliferative activity, they were generally less potent than standard monotherapies. For example, fulvestrant hybrid **7** displayed antiproliferative activity in both ER+ MCF-7 cells and in ER- MDA-MB-231 cells, but was less potent than 4-OHT (in MCF-7) or SAHA (in MDA-MB-231).³⁵

The side-chains of fulvestrant, 4-OHT, and raloxifene are responsible for their antagonist action by preventing the proper folding of H12 over the LBP and thus interfering with the recruitment of transcription cofactors. In SERDs such as fulvestrant, the long hydrophobic side chain can interact with the coactivator binding groove,⁴⁰ a capacity that correlates with induction of ER α modifications and complete transcriptional suppression.¹⁷ Thus the incorporation of polar zinc binding groups at the end of the side-chain might alter the ability of SERDs to induce ER α degradation.

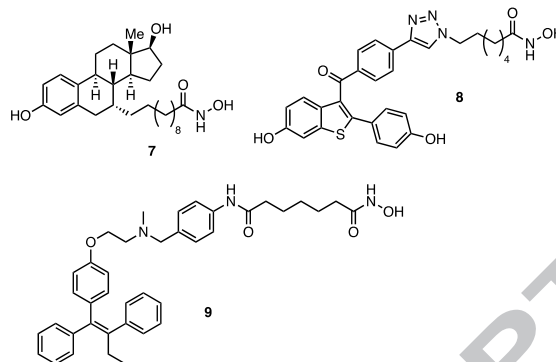


Figure 2 Structures of antiestrogen / HDACi hybrids.

2. Hybrid Design and Synthesis

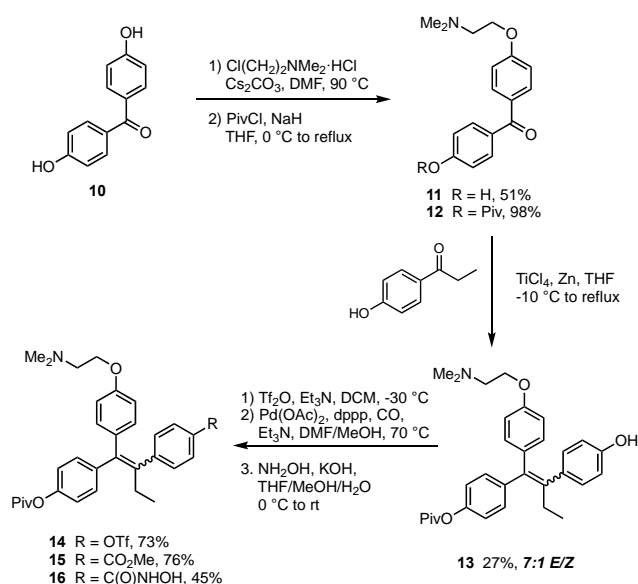
The steroidal, 4-hydroxystilbene, or 2-arylbenzothiophene cores of antiestrogens mainly provide affinity for the LBP. We have observed with vitamin D/HDACi hybrids that groups that provide HDACi function can be accommodated by the LBP of the vitamin D receptor (VDR).⁴¹⁻⁴⁴ Given the similarity between nuclear receptor binding pockets we therefore postulated that it might be possible to incorporate HDACi function into the core of an antiestrogen without significantly affecting affinity for ER α , allowing the antiestrogenic side-chain to remain unmodified and retain full functionality.⁴⁵

The phenol of 4-OHT mimics the A-ring phenol of E₂, forming hydrogen bonds to Glu353 and Arg394.⁴⁶ While E₂ possesses a second hydroxyl group in the D-ring that engages in a hydrogen bond with His524,⁴⁷ the remaining aromatic ring in 4-OHT remains unoxidized and thus appeared to be a potential position to incorporate polar functionality - indeed raloxifene places a second phenolic OH in this vicinity. Additionally, while many residues lining the ER α binding pocket show little positional variation among X-ray crystal structures of various estrogens and antiestrogens, His524 is mobile and can accommodate different positioning of hydroxyl groups, as in raloxifene,⁴⁸ and bulkier groups as in 2-arylindole antagonists.⁴⁹ We sought to exploit this flexibility by developing hybrids which attach HDACi function to the B-ring of 4-OHT. The potential advantage of this design is that it would not require alteration of the side-chain that is essential for antiestrogen function. Moreover, metabolic inactivation of the HDACi unit would not be expected to alter the antiestrogenic character of the molecules.

The hybrids were prepared using two separate routes. Hybrid BMW-275 (**16**) was prepared using a McMurry cross-coupling strategy.⁵⁰ Mono-alkylation of symmetrical benzophenone **10** followed by acylation with pivaloyl chloride provided ketone **12** in 50% yield. McMurry cross-coupling with 4'-hydroxypropionophenone provided alkene **13** as a 7:1 *E/Z* mixture. Triflation under standard conditions and then palladium-catalyzed carboxylation afforded **15** in 55% yield over 2 steps. Finally, treatment of the methyl ester with hydroxylamine and KOH afforded hydroxamic acid **16** in 45% yield.

The remaining hybrids were prepared via a three-component, nickel-catalyzed alkyne/Grignard/halide coupling.⁵¹ Treatment of aryl butyne **18** with an appropriately substituted aryl Grignard and aryl iodide in the presence of NiCl₂•6H₂O afforded alkene **19** as a single alkene stereoisomer. Unfortunately, unlike tamoxifen, the alkene in **19**, and its derivatives, is highly prone to isomerization, particularly under acidic conditions including purification by silica gel chromatography. For instance, simple removal of the TBS group in **19** with NaOH in methanol

followed by workup and silica gel chromatography afforded **20** as a 1:1 *E/Z* mixture. This propensity to isomerize presumably arises from the additional electron donating groups on the aryl rings not present in the parent tamoxifen.⁵² We thus proceeded with the 1:1 mixture and separated alkene isomers by HPLC



Scheme 1 Synthesis of hybrid **16** using a McMurry cross-coupling strategy.

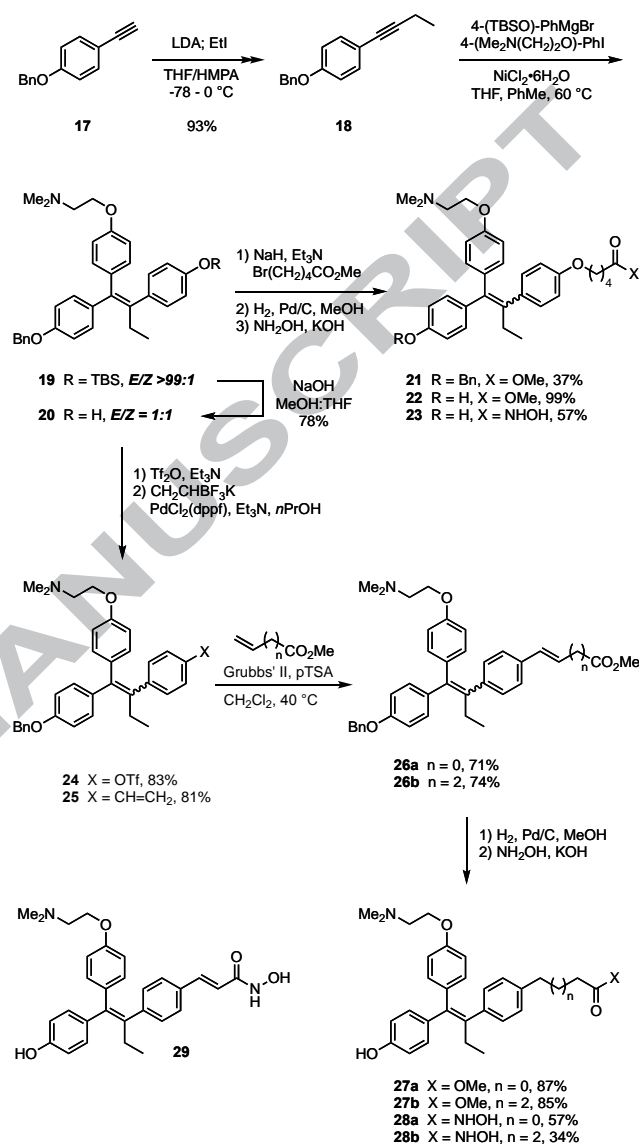
upon completion of the syntheses. Treatment of **20** with NaH and methyl 5-bromopentanoate followed by hydrogenolytic cleavage of the benzyl protecting group and hydroxamate formation, as above, afforded AFP-277 (**23**) in 21% yield over three steps.

Alternatively, triflation of **20** followed by Suzuki-Miyaura cross-coupling afforded styrene **25** in excellent yield. Cross metathesis with either methyl acrylate or methyl 4-pentenoate using Grubbs' second-generation catalyst proceeded cleanly to afford alkenes **26a/b** in good yield. Subsequent treatment with H₂/Pd-C resulted in alkene hydrogenation and hydrogenolysis of the benzyl protecting group. Finally, treatment with hydroxylamine afforded hybrids AFP-345 (**28a**) and AFP-477 (**28b**) in 35% and 21% yield, respectively, over three steps. Finally, hybrid AFP-458 (**29**) bearing a cinnamate unit could be prepared in an analogous sequence to **27a** by using a paramethoxybenzyl protecting group to avoid the need for hydrogenolysis conditions (see Supporting Information).

3. Biochemical Analysis

The antiestrogenic activity of the hybrids was first assessed using a bioluminescence resonance energy transfer (BRET) assay used previously to characterize our fulvestrant hybrids (Figure 3).³⁵ This assay measures recruitment of a coactivator (SRC1) receptor-interacting domain fused to a YFP by ERα fused to Renilla Luciferase (RLucII) via energy transfer between the two luminescent proteins in live transfected HEK293T cells. Thus, the BRET assay reflects the activity of the receptor in live cells in real time, avoiding effects on receptor expression levels caused by HDACi activity in luciferase assays. As expected, the agonist E2 (5 nM) increased net BRET values. The hybrids were initially assessed at 10 μM in the absence and presence of 5 nM E2 (Figure 3A). All hybrids displayed antiestrogenic behaviour, with **28b** most closely approaching the effectiveness of 4-OHT in suppressing SRC1 recruitment in the presence of E2. Importantly, in the absence of E2, all hybrids were devoid of partial agonist activity, in every case suppressing fluorescence

below basal levels (Figure 3A). Titration curves in the presence of E2 showed that hybrids **23**, **28a**, and **28b** all fully inhibited ERα function (Figure 3B). While none of these hybrids were more potent than 4-OHT, only a minimal loss of potency was



Scheme 2. Synthesis of hybrids **23** and **27a/b** using a nickel-catalyzed three-component cross-coupling strategy.

observed, with **23** and **28b** maintaining sub-micromolar potency. Hybrid **16** also fully inhibited ERα, but unlike hybrids **23** and **28a/b**, **16** was less potent than 4-OHT (see Supporting Information). In contrast, cinnamyl hydroxamic acid **29** displayed only partial inhibition of cofactor recruitment by ERα in the presence of E2 at the highest concentration tested. These results clearly demonstrate that it is possible to incorporate HDACi function into the B-ring of 4-OHT while maintaining ERα antagonist function but that efficacy is structure-dependent.

HDACi activity was assessed in vitro using a standard fluorometric assay.⁵³ Initial screening was carried out against HDAC6, a class IIa HDAC (Table 1). Hybrids **23**, **28a/b**, and **29** were within one order of magnitude potency of SAHA, with low μM or high nM IC₅₀ value. Hybrid **28b** was the most potent with an IC₅₀ of 300 nM. Hybrids **23**, **28a/b** and **29** were further screened against HDAC3, an example of a Class I HDAC. All hybrids were again effective, with **28b** being the most potent

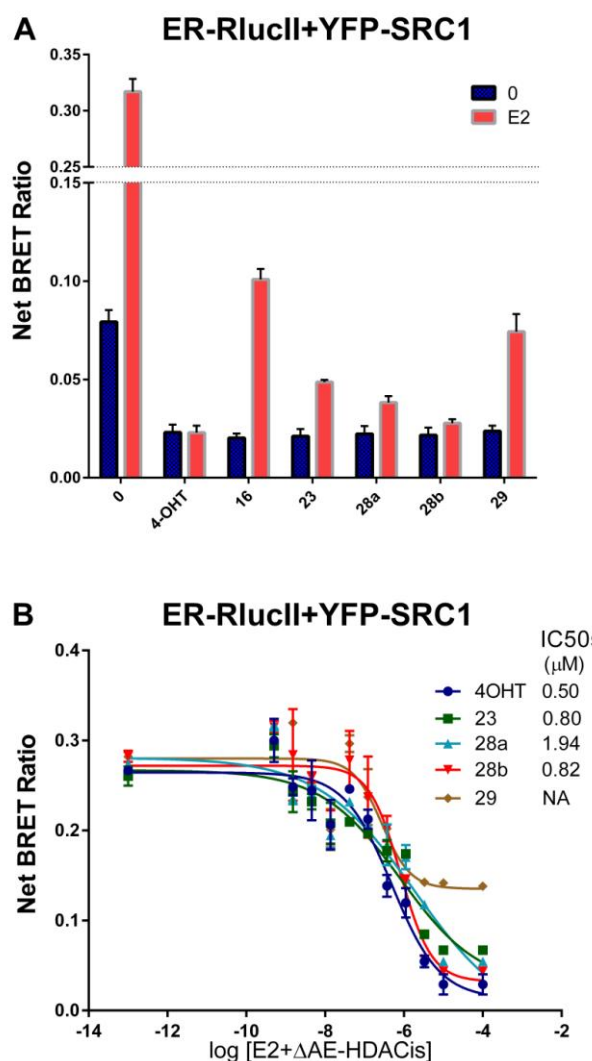


Figure 3. Antiestrogenic activity of AE-HDACi hybrid in the presence and absence of E2 in BRET assays. A) HEK293T cells were co-transfected with a constant amount of ER α -RLucII and/or YFP-SRC1. After 48 h, cells were treated with E2 (5 nM) and/or 4-OHT or AE/HDACi hybrids (10 μM) for 1 h. Transfer of energy between ER α -RLucII and YFP-SRC1 was measured in a BRET assay. B) Dose response curves were performed in HEK293T cells co-transfected with a constant amount of ER α -RLucII and YFP-SRC1. After 48 h, cells were treated with E2 (5 nM) and/or increasing amounts of 4-OHT and AE/HDACi hybrids for 1 h. A-B: Graphs represent the mean \pm SEM of data from 2 independent biological replicates.

with an IC₅₀ of 734 nM - again within an order of magnitude of SAHA. Hybrid **16**, which displayed only partial antiestrogenic activity, was also a poor HDACi (see Supporting Table S1), presumably due to the lack of a linker between the tamoxifen core and the hydroxamic acid. These assays clearly establish that attachment of short chain hydroxamic acids directly to the 4-OHT core is capable of producing viable, potent HDAC inhibitors.

With the bifunctionality of the hybrids established, the antiproliferative and cytotoxic activity of **23**, **28a/b**, and **29** were tested in CellTiter-Glo cell viability assays. In ER+ MCF-7 cells, 4-OHT displays antiproliferative effects at low concentrations relative to untreated cells (Figure 4). These effects are more marked at day 7, with cells being essentially growth-arrested

Table 1. HDACi activity of hybrids^a

Compound	HDAC6 (μM)	HDAC3 (μM)
6	0.060	0.110
23	1.78	2.10
28a	0.484	2.01
28b	0.300	0.734
29	0.519	6.72

a) Determined in a fluorometric assay using *N*-Ac-Leu-Gly-(ϵ -*N*-Ac)-Lys-AMC as substrate.

between day 4 and 7. Furthermore, 4-OHT is cytotoxic at 5-10 μM resulting in full loss of cell viability. SAHA is less antiproliferative at sub-micromolar concentrations, but inhibited cell survival more efficiently than 4-OHT in the micromolar range.

All hybrids tested had antiproliferative effects in the nanomolar range, with **23**, **28a**, and **28b** approximating the effect of 4-OHT and being more antiproliferative than SAHA over both 4 and 7-day treatment. The antiproliferative effect in that concentration range was weakest at 7 days for **29**, potentially

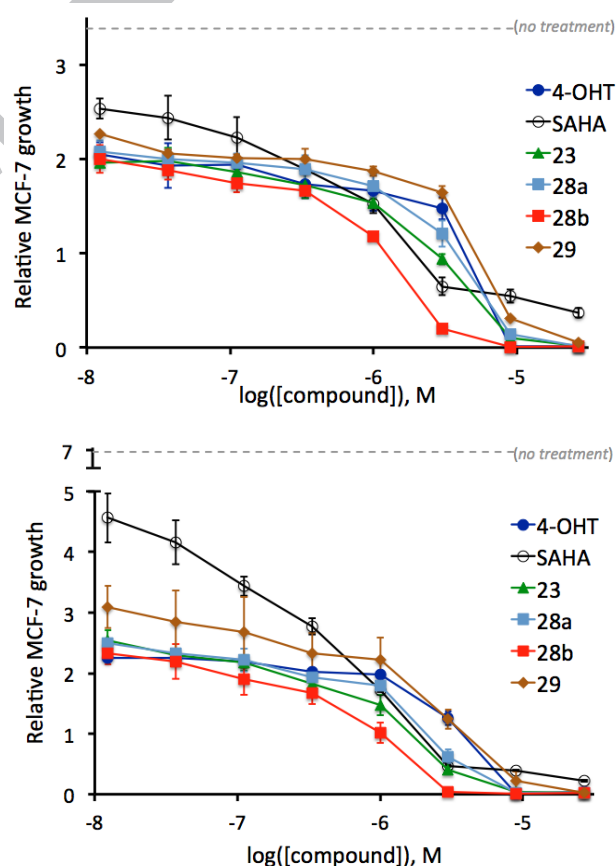


Figure 4. Antiproliferative activity in MCF-7. Cell proliferation assay in MCF-7 cells treated for 4 (top) and 7 (middle) days with either 4-OHT, SAHA, **23**, **28a**, **28b**, or **29**. All hybrids tested except for **29** have an anti-proliferative effect similar to that of 4-OHT at sub-micromolar concentrations. **28b** is more potent than 4-OHT or SAHA alone in triggering cytotoxicity. Relative MCF-7 growth was calculated by dividing the luminescent signal at day 7 over that at day 0. Values represent the means of 2 independent experiments and error bars are the SEM.

reflecting its reduced potency at suppressing ER α activation. Hybrids **23**, **28b**, and, to a lesser extent **28a**, displayed cytotoxic activity in the micromolar range at lower concentrations than 4-OHT, likely reflecting their incorporated HDACi activity. **28b** displayed the lowest IC₅₀ for cytotoxicity among all hybrids, in keeping with its superior HDACi activity (Supporting Table S2). The resulting bimodal antiproliferative profile of **28b** is thus improved with respect to either 4-OHT or SAHA alone, particularly for **28b** in the high nM to low μ M concentration range over both 4 and 7 days. This is notable as **28b** was less potent than either 4-OHT or SAHA in single-target assays and thus highlights the potential combinatorial effects of the hybrid structures.

We also assessed the efficacy of **28b** in ER α - cell lines. In triple negative MDA-MB-231 cells, neither **28b** nor 4-OHT showed antiproliferative activity at nanomolar concentrations, in keeping with the lack of ER-dependency for cell proliferation. **28b** displayed cytotoxicity in the micromolar range with an IC₅₀ intermediate between that of SAHA and 4-OHT over a 7-day course of treatment (Figure 5 and Supporting Table S3). The lower potency of **28b** relative to SAHA is in keeping with its lower HDACi potency. Similar behaviour of **28b**, i.e. cytotoxic activity in the micromolar range intermediate between that of SAHA and 4-OHT, was observed in ER α - MCF-10A cells (see Supporting Figure S3).

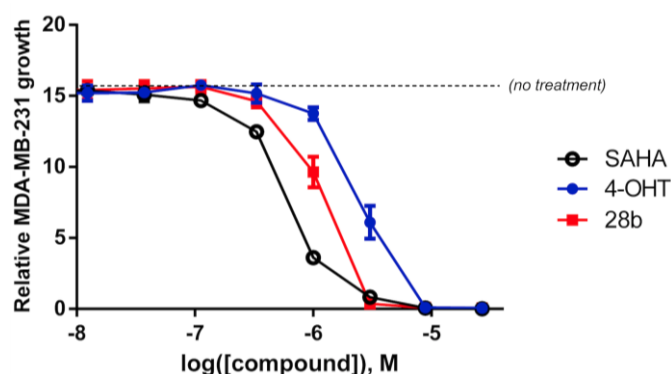


Figure 5. Antiproliferative activity in MDA-MB-231 cells. Cells were treated for 7 days with either 4-OHT, SAHA, or **28b**. Relative cell proliferation was calculated by dividing the luminescent signal at day 7 over that at day 0. Values represent the means of 3 independent experiments and error bars are the SEM.

The high potency of **28b** in the BRET and HDACi assays, and its effectiveness in the antiproliferative assays spurred a more in-depth examination of its properties, including its effects on

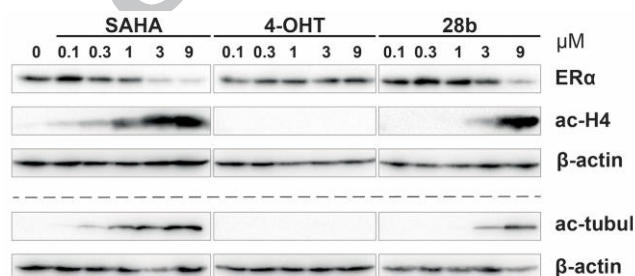


Figure 6. HDACi activity in MCF-7 cells. Cells were treated for 8 h with different concentrations of 4-OHT, SAHA or **28b**. Acetylation of histones H4 and of α -tubulin in the presence of different doses of SAHA, 4-OHT or **28b** was analyzed by Western blotting with antibodies against the corresponding acetylated proteins. ER α protein levels were also assessed. Results are representative of 2 experiments. Upper and lower Western blots (separated by the dashed line) are from two different gels loaded from identical samples.

HDAC target proteins and on ER and HDAC target genes in cells. Western blotting of MCF-7 cells treated with **28b** or SAHA both showed dose-dependent hyperacetylation of histone H4 and tubulin, consistent with its HDACi functionality (Figure 6). SAHA was slightly more potent, with effects being observed at 1 μ M vs. 3 μ M for **28b**. As expected, 4-OHT had no significant effect on acetylation of either histone H4 or tubulin. In addition, Western analysis also revealed a decrease in ER α protein levels upon treatment by either SAHA or **28b** (Figure 6), consistent with previous reports that treatment with HDACi's suppresses both ER α RNA and protein levels.⁵⁴⁻⁵⁷

Assessment of gene expression levels in MCF-7 by RT-qPCR also showed regulation patterns consistent with both ER antagonism and HDACi activity. At 5 μ M, **28b**, like SAHA but not 4-OHT, suppressed *ESR1* mRNA levels (Figure 7, top panel), consistent with the loss of ER α protein levels described above. Accordingly, expression of estrogen target genes *TFF1*, *GREB1*, and *MYC* was suppressed by **28b** in a manner similar to both SAHA and 4-OHT (Figure 7, top panel). Hybrid **28b** also induced expression of *SREBF1*, *CTGF*, and *CDKN1A*, which are induced by acetylation or HDACi treatment⁵⁸⁻⁶⁰ but only mildly affected by 4-OHT (Figure 7, bottom panel), supporting the bi-functionality of the molecule. Finally, expression of several proliferative genes including *E2F1*, *MKI67*, *MYBL2*, *CCND1*, and *CDC6* was suppressed by **28b** as well as either 4-OHT or SAHA, with similar or intermediate efficacies, in keeping with its anti-proliferative activity in MCF-7 cells (Figure 7, top panel).

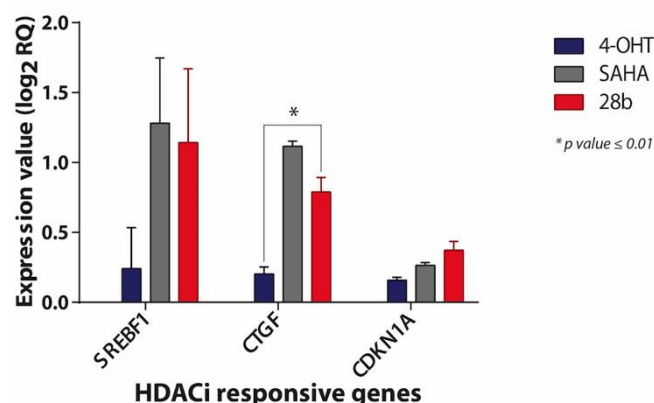
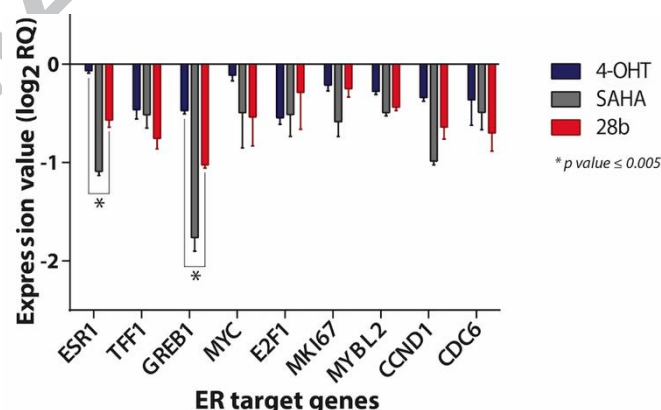


Figure 7. Hybrid **28b** regulates both ER target genes and SAHA responsive genes. MCF-7 cells were treated for 24 h with either 4-OHT, SAHA, or **28b** (5 μ M). Indicated genes were tested by RT-qPCR. Expression levels were normalized to those of the *RPLPO*, *TBP* and *YWHAZ* house-keeping genes. Values represent the means of 2 independent experiments and error bars are the SEM. *p-values were calculated with a Holm-Šidák t-test.

4. Computer Docking and Discussion

The data above clearly show that while all hybrids were bifunctional to some extent, **28b** displayed a superior combination of ER antagonist, HDACi and antiproliferative activity. The ability of hybrids **23**, **28a**, and **28b** to act as effective antagonists for the ER suggests that the ER LBP can accommodate the additional HDACi functionality in the portion of the pocket where the D-ring of E2 binds. To examine potential binding modes, we docked the hybrids in ER α crystal structures from its complexes with 4-OHT (PDB: 3ERT)^{46, 49} and a larger 2-arylindole (PDB: 2IOG) using FITTED,^{61, 62} a docking platform that has performed well in other nuclear receptor ligand hybrid studies.^{35, 63, 64} None of the hybrids docked well into the 4-OHT crystal structure - the phenol in the hybrids did not overlap with that found in 4-OHT and docking scores were quite low. In contrast, the expanded pocket in the 2-arylindole/ER structure easily accommodated the hybrids. The structure of **28b** (Figure 8) shows the hydroxamate side chain occupying a space that is present in the 2-arylindole/ER crystal structure but not in the 4-OHT/ER α structure. While these docking solutions are crystal structure-dependent, in combination with the experimental data they suggest that the ER is sufficiently flexible to adapt to the hybrid ligands.

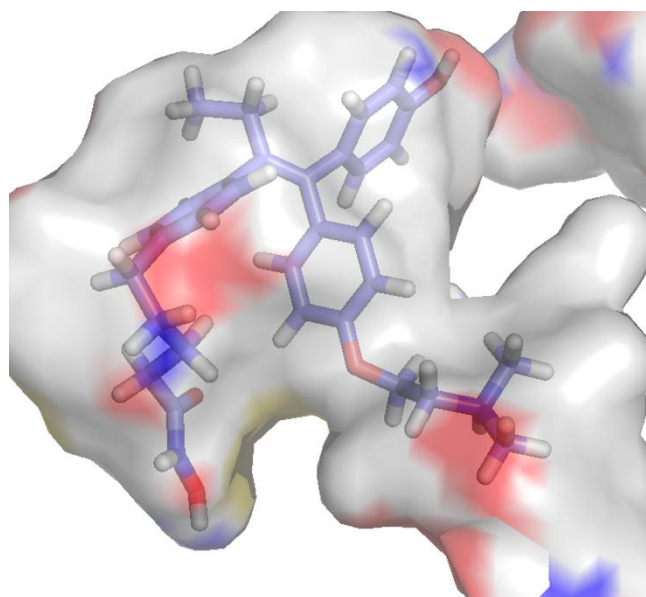


Figure 8. AFP-477 (**28b**) docked to the crystal structure of ER α derived from its complex with a 2-arylindole (PDB: 2IOG). The hydroxamate chain occupies a space (lower left) that is not present in the x-ray structure of 4-OHT bound to ER α (PDB 3ERT).

We also docked the hybrids to HDAC6 (PDB: 5EDU).⁶⁵ While hybrids **23**, **28a/b**, and **29** all easily docked with tight coordination of the hydroxamic acid to the active site zinc, the proximity of the aromatic ring in hybrid **16** prevented the hydroxamic acid from fully entering the active site (Figure 9). This was consistent with the relatively poor potency of **26** and suggests that a minimum linker of at least 2 atoms is necessary for efficient binding.

The hybrids described here represent a new design motif for bifunctional antiestrogens. Most prior examples have focused on incorporating secondary functionality in the side-chain of antiestrogens, including HDACi and cytotoxic functionalities.^{35, 37, 38, 66-68} The results herein suggest that the LBP of ER α is sufficiently pliable to accommodate larger groups while maintaining both high affinity and antagonist behavior. Similar plasticity has been observed in the VDR where Gemini ligands

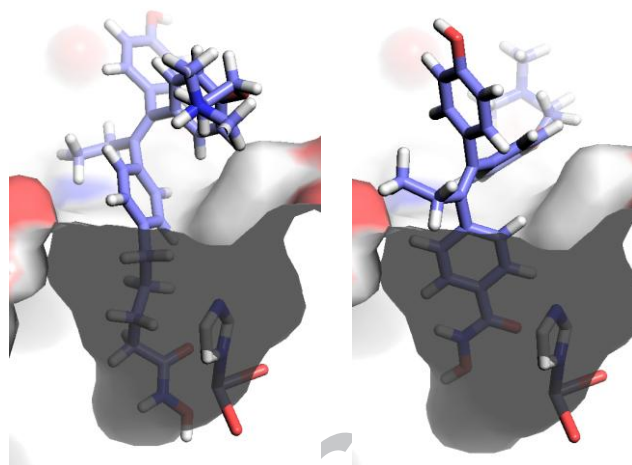


Figure 9. Comparison of docking solutions of **28b** (left) and **16** (right) to HDAC 6 (PDB:5EDU) showing improved coordination to zinc by **28b**. Zinc coordinated to His651, Asp 649 and Asp 742 in lower left.

bearing a branched chain are accommodated without losing VDR agonist function and with only minor losses in potency.⁶⁹ Compared to our prior hybrid **9**,³⁵ hybrid **28b** displays an excellent combination of antiestrogenicity and HDACi activity that leads to an improved antiproliferative profile; the molecule is as effective as 4-OHT at low concentration and more cytotoxic than either SAHA or OHT, even though it is only 1/10th as potent towards HDAC3 and 6. Future studies will examine the activity profile of these hybrids using *in vivo* models, including their uterotrophic activity, and further explore their modes of interaction with ER in structural studies.

5. Experimental Section

Unless otherwise stated, reactions were conducted under an argon atmosphere and glassware was oven dried prior to use. Tetrahydrofuran and diethyl ether were purified by distillation from sodium under a nitrogen atmosphere. Toluene, dichloromethane and triethylamine were purified by distillation from calcium hydride under nitrogen atmosphere. Deuterated chloroform was stored over activated 4 Å molecular sieves. All commercial reagents and solvents were used as purchased without further purification. Thin-layer chromatography (TLC) was carried out on glass-backed Ultrapure silica TLC plates (extra hard layer, 60 Å, thickness: 250 µm, saturated with F-254 indicator). Flash column chromatography was carried out on 230-400 mesh silica gel (Silicycle) using reagent grade solvents. Infrared (IR) spectra were obtained using Nicolet Avatar 360 FT-IR infrared spectrophotometer and data are reported in cm⁻¹. Proton and carbon nuclear magnetic resonance spectra were obtained on Varian 300, 400, and 500 or Bruker 400 and 500 MHz spectrometers. Chemical shifts (δ) were internally referenced to the residual proton resonance CDCl₃ (δ 7.26 ppm), CD₃OD (δ 3.31 ppm), (CD₃)₂SO (δ 2.50 ppm). Coupling constants (*J*) are reported in Hertz (Hz). HPLC Analysis was performed using a Waters ALLIANCE instrument (e2695 with 2489 UV detector and 3100 mass spectrometer). HRMS were obtained by Dr. Nadim Saadeh or Dr Alexander S. Wahba at McGill University Department of Chemistry

(4-(2-(Dimethylamino)ethoxy)phenyl)(4-hydroxyphenyl)methanone (11): Cs₂CO₃ (8.55 g, 26.3 mmol, 4.0 eq.) was added to a solution of 4,4'-hydroxybenzophenone **10**

(1.41 g, 6.56 mmol, 1.0 eq.) in dry DMF (15 mL) at room temperature. The mixture was heated to reflux and stirred for 10 min, at which point the solution was cooled to room temperature and *N,N*-dimethyl-2-chloro-*N,N*-dimethylethylamine hydrochloride (945 mg, 6.56 mmol, 1.0 eq.) was added portionwise. The reaction was then heated to 80 °C and stirred for 4 h, whereupon it was cooled to room temperature, quenched with saturated ammonium chloride solution (10 mL) and extracted with ethyl acetate (3 x 25 mL). The crude product was purified by column chromatography eluting with 10% MeOH in CH₂Cl₂ to afford **11** as a white solid (960 mg, 3.37 mmol) in 51% yield. The spectroscopic data of the product is in agreement with that reported in the literature.⁷⁰

4-(4-(2-(Dimethylamino)ethoxy)benzoyl)phenyl pivalate (12): NaH (60% in mineral oil, 200.3 mg, 5.01 mmol, 1.5 eq.) was added to a solution of **11** (952 mg, 3.34 mmol, 1.0 eq.) in THF (15 mL) and the resulting bright yellow suspension was stirred for 15 min. The reaction mixture was cooled to 0 °C and pivaloyl chloride (493 µL, 4.01 mmol, 1.2 eq.) was added dropwise. The reaction was warmed to room temperature and stirred for 1 h, whereupon it was quenched with distilled water (10 mL) and extracted with ethyl acetate (3 x 25 mL). The organic layers were dried over anhydrous sodium sulfate, filtered and concentrated to afford **12** as a white solid (1.22 g, 3.27 mmol) in 98% yield. ¹H NMR (400 MHz, CDCl₃) δ 7.80 (dd, *J* = 8.8, 3.0 Hz, 4H), 7.17 (d, *J* = 8.7 Hz, 2H), 6.98 (d, *J* = 8.9 Hz, 2H), 4.14 (t, *J* = 5.7 Hz, 2H), 2.76 (t, *J* = 5.7 Hz, 2H), 2.35 (s, 6H), 1.38 (s, 9H). ¹³C NMR (126 MHz, CDCl₃) δ 194.5, 176.7, 162.4, 154.0, 135.5, 132.5, 131.3, 130.2, 121.4, 114.1, 66.0, 58.0, 45.8, 39.2, 27.1. IR (film) = 3661, 2973, 2873, 2822, 2773, 1751, 1650, 1599, 1508, 1479, 1460, 1304, 1276, 1253, 1202, 1161, 1104, 1029, 928, 898, 846, 762. HRMS calc. for C₂₂H₂₈NO₄ (M+H)⁺: 370.2001. Found: 370.2013.

(E/Z)-4-(1-(4-(2-(Dimethylamino)ethoxy)phenyl)-2-(4-hydroxyphenyl)but-1-en-1-yl)phenyl pivalate (13): Titanium (IV) chloride (1.76 mL, 16.1 mmol, 4.0 eq.) was added to a suspension of zinc dust (2.11 g, 32.2 mmol, 8.0 eq.) in THF (12 mL) at 0 °C. The resulting deep brown slurry was stirred at reflux for 3h, whereupon the reaction mixture was cooled to 0 °C and ketone **12** (1.49 g, 4.02 mmol, 1.0 eq.) and 4'-hydroxypropiophenone (1.82 g, 12.1 mmol, 3.0 eq.) in THF (20 mL) were added simultaneously to the solution. The reaction mixture was stirred in the dark at reflux for 3 h, then cooled to 0 °C and quenched with 10% K₂CO₃ (50 mL). The mixture was filtered and the filtrate was extracted with ethyl acetate (3 x 50 mL). The organic layers were dried over anhydrous sodium sulfate, filtered and concentrated. The crude product was purified by column chromatography eluting with 8-16% MeOH in CH₂Cl₂ to afford **13** as a beige foam (534 mg, 1.1 mmol) in 28% yield as a 7:1 mixture of *E/Z* isomers. ¹H NMR (500 MHz, CD₃OD) δ 7.21 (d, *J* = 8.6 Hz, 2H), 7.02 (d, *J* = 8.6 Hz, 2H), 6.92 (d, *J* = 8.7 Hz, 2H), 6.78 (d, *J* = 8.9 Hz, 2H), 6.59 (d, *J* = 8.4 Hz, 4H), 3.97 (t, *J* = 5.4 Hz, 2H), 2.73 (t, *J* = 5.4 Hz, 2H), 2.42 (q, *J* = 7.4 Hz, 2H), 2.32 (s, 6H), 1.35 (s, 9H), 0.91 (t, *J* = 7.4 Hz, 3H). ¹³C NMR (126 MHz, CD₃OD) δ 177.3, 156.6, 155.5, 149.7, 141.6, 141.5, 136.7, 135.9, 133.0, 131.6, 130.5, 130.1, 120.8, 114.4, 113.1, 64.7, 57.6, 44.3, 38.7, 28.4, 26.1, 12.6. film *v* = 3449, 2966, 1750, 1607, 1508, 1478, 1397, 1275, 1240, 1197, 1164, 1116, 1029, 831, 590. HRMS calc. for C₃₁H₃₈NO₄ (M+H)⁺: 488.2795. Found: 488.2782.

(E/Z)-4-(1-(4-(2-(Dimethylamino)ethoxy)phenyl)-2-(4-(((trifluoromethyl) sulfonyl)oxy)phenyl)but-1-en-1-yl)phenyl pivalate (14): Triethylamine (34.3 µL, 0.246 mmol, 1.2 eq.) and triflic anhydride (41.3 µL, 0.246 mmol, 1.2 eq.) were added

dropwise to a solution of **13** (99.8 mg, 0.206 mmol, 1.0 eq.) in CH₂Cl₂ (5 mL) at -30 °C. The reaction mixture was stirred at -30 °C for 2 h, whereupon additional triethylamine (68.6 µL, 0.492 mmol) and triflic anhydride (82.6 µL, 0.492 mmol) were added and the solution was stirred at -30 °C for another 3 h. The reaction was quenched with distilled water (5 mL) and extracted with ethyl acetate (3 x 10 mL). The combined organic layers were dried, filtered and concentrated. Purification by column chromatography eluting with 5% MeOH in CH₂Cl₂ afforded **14** as a bright yellow product (93.8 mg, 0.151 mmol) in 73% yield as a 5:1 mixture of *E/Z* isomers. ¹H NMR (500 MHz, CD₃OD) δ 7.26 (t, *J* = 9.0 Hz, 2H), 7.16 (d, *J* = 8.8 Hz, 2H), 7.06 (d, *J* = 8.6 Hz, 2H), 6.78 (d, *J* = 8.8 Hz, 2H), 6.63 (d, *J* = 8.8 Hz, 2H), 3.99 (t, *J* = 5.4 Hz, 2H), 2.76 (t, *J* = 5.3 Hz, 2H), 2.51 (q, *J* = 7.6 Hz, 2H), 2.34 (s, 6H), 1.36 (s, 9H), 0.94 (t, *J* = 7.5 Hz, 3H). ¹³C NMR (126 MHz, CD₃OD) δ 177.3, 157.1, 153.2, 150.1, 147.9, 143.2, 140.5, 140.1, 139.2, 134.9, 131.6, 131.5, 130.0, 121.0, 120.4, 114.0, 113.3, 64.7, 57.5, 44.2, 38.7, 28.2, 26.0, 12.3. HRMS calc. for C₃₂H₃₇NO₆ (M+H)⁺: 620.2288. Found: 620.2284.

(E/Z)-Methyl-4-(1-(4-(2-(dimethylamino)ethoxy)phenyl)-1-(4-(pivaloyloxy) phenyl)but-1-en-2-yl)benzoate (15): In a flame-dried Schlenk bomb, triethylamine (17.5 µL, 0.125 mmol, 3.0 eq.) was added dropwise to a solution of **14** (25.9 mg, 41.8 µmol, 1.0 eq.) in DMF (2 mL) at room temperature. Pd(OAc)₂ (3.8 mg, 17 µmol, 0.40 eq.), 1,3-bis(diphenylphosphino)propane (5.2 mg, 13 µmol, 0.30 eq.) and MeOH (1.5 mL) were added sequentially to the solution and the flask was charged with 4 atm. carbon monoxide. The reaction mixture was heated to 70 °C and stirred overnight (18 h), after which it was cooled to room temperature and the carbon monoxide was vented. The mixture was diluted with distilled water (5 mL), extracted with ethyl acetate (3 x 10 mL) and rinsed with brine (4 mL). The organic layers were dried over anhydrous sodium sulfate, filtered and concentrated to yield an orange oil. Purification by column chromatography eluting with 3% MeOH in CH₂Cl₂ afforded **15** as a clear, colorless oil (16.8 mg, 31.7 µmol) in 76% yield as a 7:1 mixture of *E/Z* isomers (note: some 1,3-bis(diphenylphosphino)propane co-eluted with **15** and yield is calculated from HNMR analysis). ¹H NMR (400 MHz, CD₃OD) δ 7.87 – 7.76 (m, 2H), 7.33 – 7.19 (m, 4H), 7.14 – 7.02 (m, 2H), 6.79 (dd, *J* = 8.6, 2.0 Hz, 2H), 6.68 – 6.56 (m, 2H), 3.95 (q, *J* = 3.6 Hz, 2H), 3.85 (d, *J* = 1.8 Hz, 3H), 2.78 – 2.66 (m, 2H), 2.62 – 2.45 (m, 2H), 2.31 (d, *J* = 2.0 Hz, 6H), 1.37 (d, *J* = 1.9 Hz, 8H), 0.93 (td, *J* = 7.4, 1.9 Hz, 3H). ¹³C NMR (126 MHz, CD₃OD) δ 177.3, 167.1, 157.0, 149.1, 147.8, 141.0, 140.6, 138.9, 135.1, 131.6, 131.0, 129.7, 128.8, 127.7, 120.9, 113.3, 64.6, 57.5, 51.0, 45.0, 38.7, 28.1, 26.0, 12.4. HRMS calc. for C₃₃H₄₀NO₅ (M+H)⁺: 530.2901. Found: 530.2904

(Z)-4-(1-(4-(2-(Dimethylamino)ethoxy)phenyl)-1-(4-hydroxyphenyl)but-1-en-2-yl)-N-hydroxybenzamide (16): Hydroxylamine (50% w/w in H₂O, 500 eq.) was added to a solution of methyl ester **15** (15.8 mg, 34.9 µmol, 1.0 eq.) in 5:1 THF:MeOH (1.8 mL). 3M KOH (58.2 µL, 0.175 mmol, 5.0 eq.) was then added dropwise at 0 °C and the mixture was warmed to room temperature and stirred until reaction completion. The reaction mixture was subsequently neutralized with 2M HCl and crude product was concentrated under reduced pressure to afford a brown residue. Purification by reverse-phase column chromatography eluting with 10-90% MeOH in H₂O afforded product **16** as an orange residue (6.6 mg, 21.1 µmol) in 45% yield (note: some 1,3-bis(diphenyl-phosphino)propane once more co-eluted with **16** and yield is calculated from HNMR analysis). Further purification by preparatory HPLC eluting with 26-40% MeCN in H₂O with 0.1% formic acid afforded the formate salt of the product as the *Z* isomer uniquely. Analytical HPLC (C18, 5%

to 100% MeCN in H₂O) indicated the product was 94% pure. ¹H NMR (400 MHz, DMSO-*d*₆) δ 7.54 (d, *J* = 8.2 Hz, 2H), 7.14 (d, *J* = 8.2 Hz, 2H), 6.96 (d, *J* = 8.3 Hz, 2H), 6.73 (d, *J* = 8.5 Hz, 2H), 6.69 (d, *J* = 8.3 Hz, 2H), 6.58 (d, *J* = 8.3 Hz, 2H), 3.87 (t, *J* = 4.7 Hz, 2H), 2.41 (d, *J* = 8.0 Hz, 2H), 2.13 (s, 6H), 0.81 (t, *J* = 7.4 Hz, 3H). ¹³C NMR (75 MHz, DMSO-*d*₆) δ 157.0, 156.7, 145.9, 139.6, 139.2, 137.8, 135.6, 134.1, 131.9, 130.5, 129.9, 126.9, 115.4, 113.9, 112.9, 65.9, 58.1, 45.9, 28.8, 13.8. HRMS calc. for C₂₇H₃₁N₂O₄ (M+H)⁺: 447.2278. Found: 447.2293.

(Z)-2-(4-(1-(4-(Benzyloxy)phenyl)-2-(4-(tert-butyl)dimethylsilyloxy)phenyl)but-1-en-1-yl)phenoxy)-N,N-dimethylethan-1-amine (19): To a solution of **18** (1.0 g, 4.23 mmol, 1.0 eq.), 2-(4-iodophenoxy)-N,N-dimethylethan-1-amine (1.48 g, 5.08 mmol, 1.2 eq.), and NiCl₂·6H₂O (10.1 mg, 0.042 mmol, 1 mol%) in PhMe (17 mL) was added slowly 4-(tert-butyl)dimethylsilyloxy)phenyl)-magnesium bromide (0.80 M solution in THF) (6.35 mL, 5.08 mmol, 1.2 eq.). The reaction was then heated to 50 °C and stirred for 24 h. The reaction was cooled, quenched with 1 mL H₂O and filtered through a silica plug eluting with EtOAc. Purification by silica gel column chromatography using a 1-9% MeOH in CH₂Cl₂ solvent gradient gave **19** as a brown oil (786 mg, 1.31 mmol) in 31% yield as the pure *Z* isomer. ¹H NMR (400 MHz, CDCl₃) δ 7.52 – 7.47 (m, 2H), 7.46 – 7.40 (m, 3H), 7.39 – 7.34 (m, 1H), 7.19 (d, *J* = 8.7 Hz, 2H), 6.99 (d, *J* = 8.6 Hz, 4H), 6.80 (d, *J* = 8.7 Hz, 2H), 6.69 (d, *J* = 8.5 Hz, 2H), 6.60 (d, *J* = 8.8 Hz, 2H), 5.11 (s, 2H), 3.99 (t, *J* = 5.8 Hz, 2H), 2.71 (t, *J* = 5.8 Hz, 2H), 2.50 (q, *J* = 7.3 Hz, 2H), 2.35 (s, 7H), 1.01 (s, 15H), 0.21 (s, 6H). ¹³C NMR (126 MHz, CDCl₃) δ 157.5, 156.6, 153.8, 140.7, 137.3, 137.1, 136.8, 136.1, 135.6, 132.0, 130.7, 128.6, 128.0, 127.6, 119.6, 114.3, 113.3, 70.1, 65.6, 58.3, 45.9, 28.9, 25.8, 18.3, 13.7, -4.4. HRMS calc. for C₃₉H₅₀NO₃Si (M+H)⁺: 608.3554. Found: 608.3567.

(E/Z)-4-(1-(4-(Benzyloxy)phenyl)-1-(4-(2-(dimethylamino)ethoxy)phenyl)but-1-en-2-yl)phenol (20): To a solution of **19** (875 mg, 1.44 mmol, 1.0 eq.) in MeOH (14 mL) was added crushed NaOH (570 mg, 14.25 mmol, 10 eq.) and the reaction was stirred overnight at room temperature. The reaction was then quenched with 5 mL H₂O. MeOH was removed *in vacuo* and the aqueous was extracted with EtOAc (3 x 15 mL), dried over Na₂SO₄, filtered, and concentrated to a brown oil. Purification by silica gel column chromatography using a 0-8% MeOH in CH₂Cl₂ solvent gradient gave **20** as a brown oil that foamed while drying under vacuum (557 mg, 1.13 mmol) in 78% yield as a 1:1 mixture of *E:Z* isomers. ¹H NMR (400 MHz, CDCl₃) δ 7.48 (d, *J* = 7.3 Hz, 2H), 7.44 – 7.27 (m, 3H), 7.18 – 7.09 (m, 2H), 7.03 – 6.89 (m, 4H), 6.79 (dd, *J* = 9.0, 2.4 Hz, 2H), 6.66 – 6.56 (m, 4H), 5.11 (s, 2H), 4.02 (t, *J* = 5.4 Hz, 2H), 2.79 (s, 2H), 2.51 – 2.39 (q, 2H), 2.37 (s, 6H), 0.93 (t, *J* = 7.4 Hz, 3H). ¹³C NMR (126 MHz, CDCl₃) δ 157.5, 157.3, 156.7, 156.3, 154.3, 154.0, 140.8, 140.6, 137.1, 136.8, 136.7, 136.4, 136.3, 134.7, 134.3, 132.0, 131.9, 130.9, 130.6, 128.6, 128.5, 128.5, 128.0, 127.9, 127.6, 127.6, 115.0, 114.9, 114.3, 114.1, 113.7, 113.4, 70.0, 69.8, 65.5, 65.0, 58.2, 58.0, 45.7, 45.4, 28.9, 13.7. HRMS calc. for C₃₃H₃₆NO₃ (M+H)⁺: 494.2690. Found: 494.2699.

Methyl (E/Z)-5-(4-(1-(4-(benzyloxy)phenyl)-1-(4-(2-(dimethylamino)ethoxy)phenyl)but-1-en-2-yl)phenoxy)pentanoate (21): To a solution of **20** (244 mg, 0.52 mmol, 1.0 eq.) in THF (3 mL) was added NaH (60% dispersion in mineral oil) (25 mg, 0.62 mmol, 1.2 eq.) followed by freshly distilled Et₃N (87 μL, 0.62 mmol, 1.2 eq.) and methyl γ-bromo valerate (112 μL, 0.78 mmol, 1.5 eq.) which had first been passed through a plug of basic alumina. The reaction was heated to 50 °C and stirred for 5 h, then cooled to room temperature and quenched with 5 mL H₂O. THF was removed *in vacuo* and the

aqueous was extracted with EtOAc (3 x 10 mL), dried over Na₂SO₄, filtered, and concentrated to a brown residue. Purification by silica gel column chromatography using a 6.5% MeOH in CH₂Cl₂ isocratic solvent system gave **21** as an orange oil (117 mg, 0.19 mmol) in 37% yield as a 1:1 mixture of *E:Z* isomers. ¹H NMR (500 MHz, CDCl₃) δ 7.56 – 7.25 (m, 12H), 7.18 (dd, *J* = 8.5, 5.2 Hz, 3H), 7.05 (dd, *J* = 8.6, 4.0 Hz, 3H), 6.98 (d, *J* = 8.7 Hz, 2H), 6.92 (d, *J* = 8.6 Hz, 2H), 6.82 (dd, *J* = 8.7, 6.4 Hz, 4H), 6.73 (d, *J* = 3.4 Hz, 2H), 6.72 – 6.65 (m, 3H), 6.61 (d, *J* = 8.7 Hz, 2H), 5.09 (s, 2H), 4.96 (s, 2H), 4.14 (t, *J* = 5.8 Hz, 2H), 4.00 (t, *J* = 5.7 Hz, 2H), 3.94 (t, *J* = 5.6 Hz, 3H), 2.82 (t, *J* = 5.6 Hz, 2H), 2.74 (t, *J* = 5.6 Hz, 2H), 2.49 (dd, *J* = 7.4, 3.8 Hz, 3H), 2.42 (d, *J* = 4.7 Hz, 9H), 2.37 (s, 6H), 1.94 – 1.76 (m, 8H), 1.01 – 0.89 (m, 6H). ¹³C NMR (126 MHz, CD₃OD) δ 173.9, 157.5, 157.4, 157.1, 156.7, 156.5, 140.6, 137.3, 137.1, 136.8, 136.7, 136.4, 136.3, 134.7, 134.7, 132.0, 131.9, 130.7, 130.6, 130.4, 128.6, 128.5, 128.0, 127.9, 127.6, 127.5, 127.4, 114.4, 114.1, 114.0, 113.9, 113.8, 113.7, 113.4, 113.3, 70.0, 69.8, 67.2, 65.7, 65.5, 60.3, 58.3, 58.2, 53.5, 51.5, 45.8, 45.7, 34.0, 33.8, 33.7, 30.9, 29.0, 28.8, 21.7, 14.3, 13.8, 13.7. HRMS calc. for C₃₉H₄₆NO₅ (M+H)⁺: 608.3370. Found: 608.3382.

General Procedure A: Hydrogenations of benzyl esters and olefins: To a solution of starting material (1.0 eq.) in MeOH (0.1 M) was added 10 wt% of 10% Pd/C. The reaction was placed under an atmosphere of H₂ using a balloon and a vent to purge the flask of all air. The reaction was stirred for 24 h upon which it was vented, filtered through Celite, and concentrated directly.

(E/Z)-5-(4-(1-(4-(2-(Dimethylamino)ethoxy)phenyl)-1-(4-hydroxyphenyl)but-1-en-2-yl)phenoxy)pentanoate (22): Prepared from **21** (82 mg, 0.13 mmol, 1.0 eq.) according to General Procedure A. The product **22** was isolated as a bright yellow oil (71 mg, 0.13 mmol) in quantitative yield as a 1:1 mixture of *E:Z* isomers and used without further purification. ¹H NMR (400 MHz, CD₃OD) δ 7.13 (d, *J* = 8.7 Hz, 1H), 7.07 – 6.98 (m, 3H), 6.94 (d, *J* = 8.7 Hz, 2H), 6.84 – 6.64 (m, 5H), 6.61 (d, *J* = 8.9 Hz, 1H), 6.44 (d, *J* = 8.7 Hz, 1H), 4.16 (dd, *J* = 5.9, 4.9 Hz, 2H), 4.05 – 3.84 (m, 3H), 2.88 (q, *J* = 5.2 Hz, 1H), 2.80 (t, *J* = 5.5 Hz, 1H), 2.53 – 2.34 (m, 10H), 1.79 (ddt, *J* = 6.8, 4.6, 2.9 Hz, 5H), 0.98 – 0.88 (m, 6H). ¹³C NMR (126 MHz, CDCl₃) δ 174.2, 174.1, 157.1, 157.0, 156.3, 155.5, 154.5, 140.1, 140.0, 137.5, 136.9, 136.4, 135.5, 135.3, 134.9, 132.1, 131.9, 130.8, 130.7, 130.6, 130.5, 115.3, 115.2, 114.7, 114.6, 114.0, 113.9, 113.8, 113.2, 67.2, 65.9, 64.9, 64.5, 58.1, 58.0, 53.5, 51.6, 45.4, 45.3, 33.8, 33.7, 29.0, 28.9, 28.8, 28.7, 21.7, 15.2, 14.3, 13.8. HRMS calc. for C₃₂H₄₀NO₅ (M+H)⁺: 518.2901. Found: 518.2909.

General Procedure B: Hydroxamic acid formation from methyl esters: To a solution of methyl ester (1.0 eq.) in 5:1 THF:MeOH at 0 °C was added hydroxylamine (50% w/w in H₂O) (500 eq.) followed by dropwise addition of cold 3M KOH (7.0 eq.). The resulting mixture was warmed to room temperature and stirred for 24 h. The reaction was neutralized with 3M HCl, extracted three times with EtOAc, dried over Na₂SO₄, filtered, and concentrated *in vacuo*. The crude mixture was purified by reverse phase column chromatography using a 10-100% MeOH in H₂O gradient. Concentration of the purified fractions *in vacuo* followed by lyophilization of residual H₂O overnight yielded the purified products.

(Z)-5-(4-(1-(4-(2-(Dimethylamino)ethoxy)phenyl)-1-(4-hydroxyphenyl)but-1-en-2-yl)phenoxy)-N-hydroxypentanamide (23): Prepared from **22** (70 mg, 0.14 mmol, 1.0 eq.) according to General Procedure B. Reverse phase purification yielded **23** as an off white solid (41 mg, 0.06 mmol) in 57% yield as a 1:1 mixture of *E:Z* isomers. Preparatory reverse

phase HPLC purification using a 12–54% MeCN in H₂O gradient and lyophilization of the desired fractions yielded the *Z* isomer of **23** as a fluffy, amorphous, white solid. Analytical HPLC (C18, 5% to 100% MeCN in H₂O) indicated the product was 96% pure. ¹H NMR (400 MHz, CD₃OD) δ 7.01 (dd, *J* = 7.9, 4.5 Hz, 5H), 6.86–6.75 (m, 5H), 6.68 (dd, *J* = 25.8, 8.3 Hz, 6H), 4.11 (s, 2H), 3.94 (s, 2H), 3.22–3.05 (m, 3H), 2.65 (d, *J* = 13.3 Hz, 7H), 2.54–2.39 (m, 4H), 1.79 (s, 6H), 0.92 (td, *J* = 7.4, 3.1 Hz, 3H). ¹³C NMR (101 MHz, CD₃OD) δ 157.3, 156.9, 154.9, 140.2, 137.6, 137.4, 134.8, 134.6, 131.7, 131.6, 130.5, 130.3, 130.2, 128.6, 114.5, 113.9, 113.8, 113.5, 113.1, 63.4, 57.0, 43.4, 28.3, 12.6. HRMS calc. for C₃₁H₃₉N₂O₅ (M+H)⁺: 519.2853. Found: 519.2858.

(E/Z)-4-(1-(4-(Benzyloxy)phenyl)-1-(4-(dimethylamino)ethoxy)phenyl)but-1-en-2-yl)phenyl trifluoromethanesulfonate (24):

To a solution of **20** (700 mg, 1.42 mmol, 1.0 eq) in CH₂Cl₂ (28 mL) at –40 °C was added freshly distilled Et₃N (297 μ L, 2.13 mmol, 1.5 eq.) followed by dropwise addition of freshly distilled Tf₂O (238 μ L, 1.42 mmol, 1.0 eq.). The reaction was stirred for 1 hour and then quenched with 200 μ L ethylenediamine followed by 30 mL H₂O. After warming to room temperature, the reaction was extracted with CH₂Cl₂ (3 x 25 mL), dried over Na₂SO₄, filtered, and concentrated to a foamy yellow oil. Purification by silica gel column chromatography using a 0–8% solvent gradient yielded **24** as a yellow oil (737 mg, 1.18 mmol) in 83% yield as a 1:1 mixture of *E:Z* isomers. ¹H NMR (400 MHz, CDCl₃) δ 7.54–7.31 (m, 12H), 7.24–7.12 (m, 6H), 7.09 (dd, *J* = 8.8, 1.8 Hz, 4H), 6.99 (d, *J* = 8.7 Hz, 2H), 6.92 (d, *J* = 8.7 Hz, 2H), 6.79–6.67 (m, 4H), 6.65 (d, *J* = 8.8 Hz, 2H), 6.59 (d, *J* = 8.8 Hz, 2H), 5.10 (s, 2H), 4.95 (s, 2H), 4.11 (t, *J* = 5.8 Hz, 2H), 3.96 (t, *J* = 5.8 Hz, 2H), 2.77 (t, *J* = 5.7 Hz, 2H), 2.68 (t, *J* = 5.8 Hz, 2H), 2.52 (dq, *J* = 7.9, 4.0 Hz, 3H), 2.38 (s, 7H), 2.32 (s, 6H), 1.01–0.88 (t, 6H). ¹³C NMR (126 MHz, CDCl₃) δ 157.8, 157.1, 147.6, 143.4, 139.5, 136.9, 135.9, 131.9, 131.9, 131.4, 130.5, 130.5, 128.6, 128.5, 128.0, 127.9, 127.6, 127.5, 120.7, 114.4, 114.2, 113.9, 113.6, 70.1, 69.9, 66.0, 65.8, 58.4, 58.3, 46.0, 45.9, 28.8, 13.6. LRMS calc. for C₃₄H₃₅F₃NO₃S (M+H)⁺: 626.22. Found: 626.2.

(E/Z)-2-(4-(1-(4-(Benzyloxy)phenyl)-2-(4-vinylphenyl)but-1-en-1-yl)phenoxy)-N,N-dimethylethan-1-amine (25): To a solution of **24** (380 mg, 0.61 mmol, 1.0 eq.) in *n*PrOH (12 mL) was added potassium vinyltrifluoroborate (97.8 mg, 0.73, 1.2 eq.), PdCl₂(dppf) (22.3 mg, 0.031 mmol, 5 mol%), and freshly distilled Et₃N (85 μ L, 0.61 mmol, 1.0 eq.). The reaction was heated to 100 °C and stirred for 24 h. After cooling to room temperature, the reaction was quenched with 5 mL H₂O, extracted with EtOAc (3 x 15 mL), dried over Na₂SO₄, filtered, and concentrated to a dark yellow oil. Purification by silica gel column chromatography using a 0–8% MeOH in CH₂Cl₂ solvent gradient yielded **25** as a yellow oil (250 mg, 0.50 mmol) in 81% yield as a 1:1 mixture of *E:Z* isomers. ¹H NMR (400 MHz, CDCl₃) δ 7.52–7.45 (m, 2H), 7.45–7.29 (m, 10H), 7.27–7.22 (m, 3H), 7.18 (dd, *J* = 8.6, 6.2 Hz, 4H), 7.11 (dd, *J* = 8.3, 3.5 Hz, 3H), 6.99 (d, *J* = 8.7 Hz, 2H), 6.93 (d, *J* = 8.7 Hz, 2H), 6.83 (dd, *J* = 8.9, 7.1 Hz, 3H), 6.67 (d, *J* = 8.8 Hz, 3H), 6.61 (d, *J* = 8.8 Hz, 2H), 5.72 (ddd, *J* = 17.6, 3.0, 1.0 Hz, 2H), 5.22 (ddd, *J* = 10.8, 2.6, 1.0 Hz, 2H), 5.11 (s, 2H), 4.96 (s, 2H), 4.13 (t, *J* = 5.8 Hz, 2H), 3.98 (t, *J* = 5.8 Hz, 2H), 2.80 (t, *J* = 5.7 Hz, 2H), 2.71 (t, *J* = 5.7 Hz, 2H), 2.52 (qd, *J* = 7.4, 3.6 Hz, 4H), 2.37 (d, *J* = 30.1 Hz, 12H), 0.97 (td, *J* = 7.5, 1.4 Hz, 6H). ¹³C NMR (126 MHz, CDCl₃) δ 157.6, 156.8, 142.4, 142.3, 140.7, 138.0, 137.1, 136.8, 136.7, 136.6, 136.4, 136.1, 135.9, 135.1, 132.0, 131.9, 131.7, 130.6, 130.4, 129.9, 128.6, 128.5, 128.3, 128.0, 127.9, 127.6, 127.5, 127.4, 126.2, 126.1, 125.8, 115.4, 114.9, 114.4, 114.1, 114.0,

113.7, 113.5, 113.4, 113.0, 70.1, 69.8, 65.9, 65.7, 58.4, 58.3, 45.9, 28.9, 13.7. HRMS calc. for C₃₅H₃₈NO₂ (M+H)⁺: 504.2897. Found: 504.2906.

Methyl (E/Z)-3-(4-((Z)-1-(4-(benzyloxy)phenyl)-1-(4-(dimethylamino)ethoxy)phenyl)but-1-en-2-yl)phenyl)acrylate (26a): To a solution of **25** (155 mg, 0.31 mmol, 1.0 eq.) in CH₂Cl₂ (1 mL) was added anhydrous PTSA (58 mg, 0.34 mmol, 1.1 eq.). The reaction was stirred at room temperature for 10 minutes until the complete dissolution of PTSA and then was concentrated *in vacuo*. To the dry residue under argon was added methyl acrylate (281 μ L, 3.1 mmol, 10 eq.), and Grubbs' gen. 2 catalyst (13.2 mg, 0.02 mmol, 5 mol%) in CH₂Cl₂ (0.5 mL). The reaction was heated to 40 °C and stirred for 24 h and then cooled to room temperature. To the reaction was again added Grubbs' gen. 2 catalyst (13.2 mg, 0.02 mmol, 5 mol%) in CH₂Cl₂ (0.5 mL) and the reaction was heated to 40 °C and stirred overnight. The reaction was cooled to room temperature, quenched with saturated NaHCO₃ (5 mL) and extracted with CH₂Cl₂ (3 x 5 mL). Purification by silica gel column chromatography using a 0–8% MeOH in CH₂Cl₂ gradient yielded **26a** as a dark brown/green oil (123 mg, 0.22 mmol) in 71% yield as a 1:1 mixture of *E:Z* isomers. ¹H NMR (400 MHz, CDCl₃) δ 7.65 (dd, *J* = 16.0, 3.0 Hz, 2H), 7.51–7.45 (m, 2H), 7.45–7.29 (m, 12H), 7.22–7.13 (m, 6H), 6.98 (d, *J* = 8.7 Hz, 2H), 6.92 (d, *J* = 8.7 Hz, 2H), 6.79 (dd, *J* = 8.7, 5.8 Hz, 3H), 6.66 (d, *J* = 8.8 Hz, 2H), 6.59 (d, *J* = 8.8 Hz, 2H), 6.39 (dd, *J* = 16.0, 2.3 Hz, 2H), 5.10 (s, 2H), 4.95 (s, 2H), 4.12 (t, *J* = 5.8 Hz, 2H), 3.97 (t, *J* = 5.7 Hz, 2H), 3.82 (s, 6H), 2.80 (t, *J* = 5.7 Hz, 2H), 2.70 (t, *J* = 5.7 Hz, 2H), 2.53 (qd, *J* = 7.4, 3.6 Hz, 4H), 2.40 (s, 6H), 2.34 (s, 6H), 0.96 (td, *J* = 7.4, 1.1 Hz, 6H). ¹³C NMR (126 MHz, CDCl₃) δ 167.6, 157.7, 157.0, 145.4, 144.8, 140.2, 138.9, 137.0, 136.3, 136.1, 135.8, 135.6, 132.0, 131.9, 130.6, 130.3, 128.6, 128.5, 128.0, 127.9, 127.8, 127.7, 127.6, 127.5, 116.9, 114.4, 114.1, 113.8, 113.5, 70.1, 69.8, 65.9, 65.7, 58.3, 51.6, 45.9, 28.8, 13.7. HRMS calc. for C₃₇H₄₀NO₄ (M+H)⁺: 562.2952. Found: 562.2965.

Methyl (E/Z)-3-(4-(1-(4-(2-(dimethylamino)ethoxy)phenyl)-1-(4-hydroxyphenyl)but-1-en-2-yl)phenyl)propanoate (27a): Prepared from **26a** (123 mg, 0.22 mmol, 1.0 eq.) according to General Procedure A. **27a** was isolated as a pale yellow oil (90 mg, 0.19 mmol) that was used without further purification in 87% yield as a 1:1 mixture of *E:Z* isomers. ¹H NMR (500 MHz, CDCl₃) δ 7.09 (d, *J* = 8.6 Hz, 2H), 7.07–6.92 (m, 10H), 6.80 (d, *J* = 7.9 Hz, 3H), 6.75–6.61 (m, 6H), 6.47 (d, *J* = 8.2 Hz, 2H), 6.39–6.32 (m, 2H), 4.10 (t, *J* = 5.6 Hz, 2H), 3.94 (t, *J* = 5.6 Hz, 2H), 3.67 (d, *J* = 4.0 Hz, 6H), 2.93–2.86 (m, 4H), 2.84 (t, *J* = 5.5 Hz, 2H), 2.75 (t, *J* = 5.6 Hz, 2H), 2.61 (td, *J* = 7.9, 5.5 Hz, 4H), 2.48 (dd, *J* = 11.1, 7.4 Hz, 6H), 2.41 (s, 6H), 2.36 (s, 6H), 0.93 (td, *J* = 7.4, 4.3 Hz, 6H). ¹³C NMR (126 MHz, CDCl₃) δ 173.6, 173.6, 157.2, 156.4, 155.8, 154.8, 140.8, 140.7, 140.2, 140.1, 138.1, 138.0, 137.8, 136.7, 136.2, 135.1, 134.8, 132.1, 131.9, 130.6, 130.5, 129.9, 129.8, 127.7, 115.4, 114.7, 113.8, 113.1, 64.9, 64.5, 58.1, 53.5, 51.6, 45.6, 45.4, 45.3, 35.7, 30.7, 30.6, 30.4, 29.0, 28.9, 27.0, 26.9, 26.6, 26.5, 26.4, 26.3, 25.3, 13.8, 13.7. HRMS calc. for C₃₀H₃₆NO₄ (M+H)⁺: 474.2639. Found: 474.2636.

(Z)-3-(4-(1-(4-(2-(Dimethylamino)ethoxy)phenyl)-1-(4-hydroxyphenyl)but-1-en-2-yl)phenyl)-N-

hydroxypropanamide (28a): Prepared from **27a** (90 mg, 0.19 mmol, 1.0 eq.) according to General Procedure B. The product was isolated as an amorphous white solid (51 mg, 0.11 mmol) in 57% yield as a 1:1 mixture of *E:Z* isomers. Subsequent preparatory reverse phase HPLC purification using a 12–54% MeCN in H₂O gradient and lyophilization of the desired fractions yielded the *Z* isomer of **28a** as a fluffy, amorphous, white solid.

Analytical HPLC (C18, 5% to 100% MeCN/H₂O) indicated the product was 96% pure ¹H NMR (500 MHz, CDCl₃) δ 8.57 (s, 3H), 7.02 (d, *J* = 8.5 Hz, 6H), 6.84 – 6.71 (m, 4H), 6.60 (d, *J* = 8.8 Hz, 2H), 4.02 (t, *J* = 5.4 Hz, 2H), 2.86 (t, *J* = 7.7 Hz, 2H), 2.80 (t, *J* = 5.4 Hz, 2H), 2.52 – 2.44 (m, 3H), 2.39 (s, 6H), 0.91 (t, *J* = 7.4 Hz, 3H). HRMS calc. for C₂₉H₃₅N₂O₄ (M+H)⁺: 475.2591. Found: 475.2594.

Methyl (E/Z)-5-(4-((Z)-1-(4-(benzyloxy)phenyl)-1-(4-(2-(dimethylamino)ethoxy)phenyl)but-1-en-2-yl)phenyl)pent-4-enoate (26b): **26b** was prepared using an identical procedure as **26a**, using a solution of **25** (148 mg, 0.29 mmol, 1.0 eq.) in CH₂Cl₂ (1 mL), anhydrous PTSA (56 mg, 0.32 mmol, 1.1 eq.), methyl 4-pentenoate (336 mg, 2.9 mmol, 10eq.), and two additions of Grubbs' gen. 2 catalyst (12.5 mg, 0.015 mmol, 5 mol%) in CH₂Cl₂ (0.5 mL). Purification by silica gel column chromatography using a 0-8% MeOH in CH₂Cl₂ gradient yielded **26b** as a dark brown/green oil (129 mg, 0.22 mmol) in 74% yield as a 1:1 mixture of *E:Z* isomers. ¹H NMR (500 MHz, CDCl₃) δ 7.48 (d, *J* = 7.0 Hz, 2H), 7.46 – 7.30 (m, 9H), 7.24 – 7.10 (m, 7H), 7.06 (td, *J* = 6.0, 3.1 Hz, 4H), 6.97 (d, *J* = 8.6 Hz, 3H), 6.91 (d, *J* = 8.6 Hz, 2H), 6.80 (ddd, *J* = 8.0, 6.4, 1.6 Hz, 4H), 6.71 – 6.62 (m, 2H), 6.59 (d, *J* = 8.7 Hz, 2H), 5.09 (s, 2H), 4.95 (s, 1H), 4.12 (t, *J* = 5.8 Hz, 2H), 3.97 (t, *J* = 6.0 Hz, 2H), 3.74 (s, 2H), 3.71 (s, 3H), 3.29 – 3.22 (m, 1H), 2.78 (s, 2H), 2.69 (s, 2H), 2.51 (td, *J* = 9.4, 8.7, 3.8 Hz, 6H), 2.39 (s, 6H), 2.33 (s, 6H), 2.00 – 1.79 (m, 6H), 1.45 (t, *J* = 10.4 Hz, 2H), 0.94 (t, *J* = 7.3 Hz, 6H). ¹³C NMR (126 MHz, CDCl₃) δ 132.0, 131.9, 130.6, 129.9, 128.6, 128.5, 128.0, 127.6, 127.5, 126.1, 125.6, 120.8, 119.2, 114.3, 114.1, 113.7, 113.4, 70.0, 69.8, 53.4, 51.6, 45.9, 27.0, 26.9, 26.4, 26.2, 13.7. HRMS calc. for C₃₉H₄₄NO₄ (M+H)⁺: 590.3265. Found: 590.3260.

Methyl (E/Z)-5-(4-(1-(4-(2-(dimethylamino)ethoxy)phenyl)-1-(4-hydroxyphenyl)but-1-en-2-yl)phenyl)pentanoate (27b): Prepared from **26b** (127 mg, 0.22 mmol, 1.0 eq.) according to General Procedure A. **27b** was isolated as a pale yellow oil (94 mg, 0.19 mmol) that was used without further purification in 85% yield as a 1:1 mixture of *E:Z* isomers. ¹H NMR (500 MHz, CDCl₃) δ 7.21 – 7.03 (m, 5H), 7.03 – 6.89 (m, 7H), 6.79 (dd, *J* = 10.8, 8.5 Hz, 4H), 6.75 – 6.60 (m, 4H), 6.53 – 6.43 (m, 2H), 6.43 – 6.34 (m, 1H), 4.10 (td, *J* = 5.7, 1.8 Hz, 2H), 3.94 (t, *J* = 5.6 Hz, 2H), 3.69 (s, 4H), 2.85 – 2.76 (m, 2H), 2.72 (t, *J* = 5.6 Hz, 2H), 2.62 – 2.43 (m, 6H), 2.43 – 2.36 (m, 5H), 2.35 – 2.24 (m, 4H), 2.00 – 1.80 (m, 6H), 1.71 – 1.53 (m, 5H), 1.44 (t, *J* = 9.4 Hz, 3H), 1.02 – 0.83 (m, 6H). ¹³C NMR (126 MHz, CDCl₃) δ 140.8, 140.6, 132.1, 131.9, 130.7, 130.6, 130.5, 129.7, 129.7, 129.6, 127.9, 127.8, 127.8, 126.3, 115.2, 114.4, 113.9, 113.1, 58.3, 53.4, 51.6, 51.5, 45.7, 45.5, 35.5, 35.0, 34.2, 34.0, 33.4, 30.7, 27.0, 26.9, 26.3, 26.1, 24.6, 13.7. HRMS calc. for C₃₂H₄₀NO₄ (M+H)⁺: 502.2952. Found: 502.2948.

(Z)-5-(4-(1-(4-(2-(Dimethylamino)ethoxy)phenyl)-1-(4-hydroxyphenyl)but-1-en-2-yl)phenyl)-N-hydroxypentanamide (28b): Prepared from **27b** (93 mg, 0.19 mmol, 1.0 eq.) according to General Procedure B. Purification by reverse phase column chromatography yielded **28b** as a white solid (33 mg, 0.06 mmol) in 34% yield as a 1:1 mixture of *E:Z* isomers. Subsequent preparatory reverse phase HPLC purification using a 12-54% MeCN in H₂O gradient and lyophilisation of the desired fractions yielded the *Z* isomer of **28b** as a fluffy, amorphous, white solid. Analytical HPLC (C18, 5% to 100% MeCN/H₂O) indicated the product was >99% pure ¹H NMR (500 MHz, CD₃OD) δ 7.07 – 6.94 (m, 6H), 6.83 – 6.73 (m, 4H), 6.62 (d, *J* = 8.4 Hz, 2H), 4.15 (t, *J* = 5.7 Hz, 2H), 3.28 (s, 2H), 2.76 (s, 6H), 2.58 (t, *J* = 6.8 Hz, 2H), 2.49 (q, *J* = 7.4 Hz, 2H), 2.10 (d, *J* = 7.5 Hz, 2H), 1.70 – 1.47 (m, 5H), 0.94 (t, *J* =

7.4 Hz, 4H). HRMS calc. for C₃₁H₃₉N₂O₄ (M+H)⁺: 503.2904. Found: 503.2912.

Cell lines and reagents:

Cell lines were purchased from the American Type Culture Collection (ATCC) and maintained in a humidified 37°C, 5% CO₂ incubator. MCF-7 cells were cultured at 37°C in alpha modification of Eagle's medium (αMEM, Wisent) supplemented with 10% Fetal Bovine Serum (FBS, Sigma), 2 mM L-glutamine and 100 UI/mL penicillin-streptomycin (Wisent). MCF-10A cells were maintained in Dulbecco's modified Eagle's F-12 media (DMEM F-12, Wisent) without calcium chloride and supplemented with 10 % FBS, 10 ng / ml epidermal growth factor (EGF), 10 µg / ml insulin, 0.5 µg / ml hydrocortisone, 100 ng / ml cholera enterotoxin (Sigma) and 100 UI/mL penicillin-streptomycin. MDA-MB-231 cells were cultured in DMEM (Wisent) supplemented with 5 % FBS and 100 UI/mL penicillin-streptomycin. HEK293T cells were maintained in DMEM supplemented with 10% FBS and 100 UI/mL penicillin-streptomycin.

The transfection reagent polyethylenimine (PEI) was ordered from Polysciences, Inc. 17β-Estradiol, 4-hydroxytamoxifen (4-OHT) and suberoylanilide hydroxamic acid (SAHA) were purchased from Sigma, Tocris and Cayman Chemical Company respectively.

Rabbit polyclonal anti-acetyl-histone H4 (06-598) and rabbit monoclonal ERα, clone 60C (04-820) were purchased from EMD Millipore. Mouse monoclonal anti-acetyl-tubulin α (ab24610) was ordered from Abcam. Mouse monoclonal anti-β-actin, clone AC-15 (A5441) was obtained from Sigma. Horseradish peroxidase (HRP)-conjugated secondary antibodies were obtained from Jackson Laboratory. Polyvinylidene difluoride (PVDF) membranes were purchased from EMD Millipore. Enhanced chemiluminescence (ECL) detection reagents were ordered from Bio-Rad.

Cell transfection: For BRET assays, HEK293T cells were maintained in DMEM (Wisent) supplemented with 10% FBS, 100 UI/mL penicillin/streptomycin, and cultured at 37°C. Before each experiment, cells were switched for 48 h in DMEM without phenol red, supplemented with 10% charcoal-dextran-treated FBS, 100 UI/mL penicillin/streptomycin and 4 mM L-glutamine. On the following day, cells were co-transfected with an expression vector for Renilla Luciferase II conjugated to the C-terminus of human ERα (pcDNA3.1-ERα-RLucII; 30 ng/million cells), either alone (for background evaluation) or together with an expression vector for YFP (Topaz) fused to aa 625-1050 of human NCOA1/SRC1 (pcDNA3.1-NCOA1-eYFP, 1.2 µg) or for two copies of YFP (Topaz) fused at the N- and C-termini of a tandem repeat of an LXXLL motif derived from NCOA2 (L peptide: KHKILHRLLODSS) and of the glucocorticoid receptor nuclear localization signal (N peptide: DRAHSTPPKKNKRNVRDPK DRAHSTPPKKNKRNVRDPK) (vector pYFP-L2N2-YFP; 1.5 µg/million cells). The amount of DNA was complemented to a total of 1.7 µg using pcDNA 3.1 (empty vector) in 75 µl of PBS/million cells. Transient transfections were performed using PEI (dissolved in water and heated up to 80°C). PEI (3 µg of linear PEI and 1 µg of polybranched PEI for each µg of DNA diluted in PBS) was mixed with DNA (1V/V, 150 µl total) and left for 15-20 min at room temperature. Cells (1 million in 850 µl) were added to the PEI:DNA mixture and were seeded (50,000 cells per well) in 96-well white plates (Costar, Corning). 48 h later, HEK293T cells were treated with hormones in triplicates. The medium was

aspirated and replaced by PBS supplemented with hormones 1 h before BRET assays.

BRET Assays: Coelenterazine H (Coel-h, Nanolight Technology) was added to each well to a final concentration of 10 μ M. Readings were then collected using a MITHRAS LB940 (Berthold Technology) multidetector plate reader, allowing the sequential integration of the signals detected in the 485/20 nm and 530/25 nm windows, for luciferase and YFP light emissions, respectively. The BRET signal was determined by calculating the ratio of the light intensity emitted by the YFP fusion over the light intensity emitted by the Luc fusion. The values were corrected by subtracting the background BRET signal detected when the Luc fusion construct was expressed alone. For BRET titration experiments, BRET ratios were expressed as a function of the [acceptor]/[donor] expression ratio (YFP/Luc). Total fluorescence and luminescence were used as a relative measure of total expression of the acceptor and donor proteins, respectively. Total fluorescence was determined with a FlexStation II microplate reader (Molecular Devices) using an excitation filter at 485/9 nm and an emission filter at 538/18 nm. Total luminescence was measured in the MITHRAS LB940 plate reader 3 min after the addition of Coel-h (10 μ M, Nanolight Technology) in the absence of emission filter. IC₅₀ values were calculated with GraphPad from 2 independent experiments (standard errors lower than 5%).

In Vitro HDAC Assays: HDAC3–“NCoR1” and HDAC6 were purchased from Cayman Chemicals and used without further purification. The HDAC assay buffer consisted of 50 mM Tris-HCl, 137 mM NaCl, 2.7 mM KCl, 1 mM MgCl₂, and bovine serum albumin (0.5 mg/mL), pH was adjusted to 8 using 6 M NaOH and 1 M HCl as needed. Trypsin [25 mg/mL, from porcine pancreas, in 0.9% sodium chloride] was from Sigma Aldrich. Stock solutions of inhibitors and substrate were obtained by dissolution in DMSO and addition of HDAC assay buffer to afford solutions containing 1.7 % v/v DMSO. Serial dilution using HDAC buffer containing 1.7 % v/v DMSO was used to obtain all requisite inhibitors and substrate solutions.

For inhibition of recombinant human HDAC3 and HDAC6, dose–response experiments with internal controls were performed in black low-binding Nunc 96-well microtiter plates. Dilution series (8 concentrations) were prepared in HDAC assay buffer with 1.7 % v/v DMSO. The appropriate dilution of inhibitor (10 μ L of 5 times the desired final concentration) was added to each well followed by HDAC assay buffer (25 μ L) containing substrate [Ac-Leu-Gly-Lys(Ac)-AMC, 40 or 30 μ M for HDAC 3 and 80 or 60 μ M for HDAC 6]. Finally, a solution of the appropriate HDAC (15 μ L) was added [HDAC3, 10 ng/well; HDAC 6, 60 ng/well] and the plate incubated at 37 °C for 30 min with mechanical shaking (270 rpm). Then trypsin (50 μ L, 0.4 mg/mL) was added and the assay developed for 30 min at room temperature with mechanical shaking (50 rpm). Fluorescence measurements were then taken on a Molecular Devices SpectraMax i3x plate reader with excitation at 360/9 nm nm and detecting emission at 460 nm/15 nm. Each assay was performed in triplicate at two different substrate concentrations. Baseline fluorescence emission was accounted for using blanks, run in triplicate, containing substrate (25 μ L), HDAC assay buffer (15 μ L), HDAC assay buffer with 1.7 % v/v DMSO (10 μ L), and trypsin (50 μ L). Fluorescence emission was normalized using controls, run in triplicate, containing substrate (25 μ L), HDAC (15 μ L), HDAC assay buffer with 1.7 % v/v DMSO (10 μ L), and trypsin (50 μ L). The data were analyzed by nonlinear regression with GraphPad Prism to afford IC₅₀ values from the dose–response experiments. K_i values were determined from the

Cheng–Prusoff equation [$K_i = IC_{50}/(1+[S]/K_m)$] with the assumption of a standard fast-on–fast-off mechanism of inhibition.

Cell proliferation assay: MCF-7 cells were plated at 300 cells per well in α MEM supplemented with 5% FBS (v/v), 2 mM L-glutamine, 100 UI/mL penicillin and 100 μ g /mL streptomycin in 384-well plates, (Corning® Costar®, Sigma). MCF-10A and MDA-MB-231 were seeded at 200 cells / well in the same media. Cells were treated every 2 days with different concentrations of either 4-OHT, SAHA, or hybrids with media replenishment after 4 days. After 7 days of treatment, cell proliferation was measured using the CellTiter-Glo® luminescent assay (Promega) following the manufacturer’s instructions. Acquisition of luminescence was performed using the Synergy NEO microplate reader (BioTek). Results were analyzed using GraphPad Prism software.

Western Blotting: MCF-7 cells were plated at 0.6 million cells per 6 cm Petri dish in α MEM supplemented with 5% FBS (v/v), 2 mM L-glutamine, 100 UI penicillin and 100 μ g/mL streptomycin. Cells were treated for 8 h and harvested in protein extraction buffer (50 mM Tris-HCl pH 7.5, 150 mM NaCl, 5 mM EDTA, 2% SDS, 0.5% Triton X-100, 1% NP-40). Proteins were loaded on SDS-PAGE gel (14%, 50 μ g protein/lane) and transferred to a PVDF membrane, then blotted overnight with primary antibodies targeting either acetyl-tubulin, acetyl-histone H4, ER α or β -actin.

Reverse transcription and Real-Time quantitative PCR: MCF-7 cells were seeded at 0.2 million cells per well of a 6-well plate and grown for 24 h in α MEM supplemented with 5% FBS (v/v), 2 mM L-glutamine, 100 UI penicillin and 100 μ g/mL streptomycin. After 24 h of treatment with either 4-OHT, SAHA or **28b** (5 μ M), cells were collected in QIAzol reagent (Qiagen) and RNA extraction was performed following manufacturer’s instructions. Total RNA (2 μ g) was reverse transcribed using the RevertAid H first minus strand cDNA synthesis kit (Fermentas). cDNA was diluted 10 times in water and used for RT-qPCR. Relative gene expression levels were evaluated using the Universal Probe Library (Roche). Amplification levels were detected with the Vii7 Real-Time PCR system (Life Technologies). All reactions have been performed in triplicates in two independent experiments. The $\Delta\Delta$ CT method was used to evaluate relative gene expression. Housekeeping genes (*RPLP0*, *TBP* and *YWHAZ*) were used as endogenous controls. For specific primers and probes used for RT-qPCR, see Supporting Information.

6. Acknowledgments

The authors thank the Canadian Institutes of Health Research for funding. S.M. holds the CIBC breast cancer research chair at Université de Montréal. A.F.P. thanks CIHR for a postgraduate fellowship. B.M.W. thanks NSERC for a postgraduate fellowship, M.D. and M.E.E. thank the Molecular Biology training program at Université de Montréal for studentships.

7. References and notes

1. Nilsson, S.; Makela, S.; Treuter, E.; Tujague, M.; Thomsen, J.; Andersson, G.; Enmark, E.; Pettersson, K.; Warner, M.; Gustafsson, J. A., *Physiol Rev* **2001**, *81*, 1535-1565.
2. Sanchez, R.; Nguyen, D.; Rocha, W.; White, J. H.; Mader, S., *Bioessays* **2002**, *24*, 244-254.

3. Ricketts, D.; Turnbull, L.; Ryall, G.; Bakhshi, R.; Rawson, N. S.; Gazet, J. C.; Nolan, C.; Coombes, R. C., *Cancer Res.* **1991**, *51*, 1817-1822.
4. Ariazi, E. A.; Ariazi, J. L.; Cordera, F.; Jordan, V. C., *Curr. Top. Med. Chem.* **2006**, *6*, 181-202.
5. Jordan, V. C.; O'Malley, B. W., *J. Clin. Oncol.* **2007**, *25*, 5815-2584.
6. Cole, M. P.; Jones, C. T.; Todd, I. D., *Br. J. Cancer* **1971**, *25*, 270-275.
7. Ward, H. W., *Br. Med. J.* **1973**, *1*, 13-14.
8. Miller, C. P., *Curr. Pharm. Des.* **2002**, *8*, 2089-2111.
9. Jordan, N. J.; Gee, J. M.; Barrow, D.; Wakeling, A. E.; Nicholson, R. I., *Breast Cancer Res. Treat.* **2004**, *87*, 167-180.
10. Adam, H. K.; Douglas, E. J.; Kemp, J. V., *Biochem. Pharmacol.* **1979**, *28*, 145-147.
11. Lim, Y. C.; Desta, Z.; Flockhart, D. A.; Skaar, T. C., *Cancer Chemother. Pharmacol.* **2005**, *55*, 471-478.
12. Early Breast Cancer Trialists' Collaborative, G., *Lancet* **2015**, *386*, 1341-1352.
13. *Lancet* **1998**, *351*, 1451-1467.
14. Shah, R.; O'Regan, R. M., *Cancer treatment and research* **2018**, *173*, 15-29.
15. Jinih, M.; Relihan, N.; Corrigan, M. A.; O'Reilly, S.; Redmond, H. P., *The breast journal* **2017**, *23*, 694-705.
16. McDonnell, D. P.; Wardell, S. E.; Norris, J. D., *J Med Chem* **2015**, *58*, 4883-4887.
17. Hilmi, K.; Hussein, N.; Mendoza-Sanchez, R.; El-Ezzy, M.; Ismail, H.; Durette, C.; Bail, M.; Rozendaal, M. J.; Bouvier, M.; Thibault, P.; Gleason, J. L.; Mader, S., *Mol. Cell. Biol.* **2012**, *32*, 3823-3837.
18. Traboulsi, T.; El Ezzy, M.; Gleason, J. L.; Mader, S., *J Mol Endocrinol* **2017**, *58*, R15-R31.
19. Chia, S.; Gradishar, W.; Mauriac, L.; Bines, J.; Amant, F.; Federico, M.; Fein, L.; Romieu, G.; Buzdar, A.; Robertson, J. F.; Brufsky, A.; Possinger, K.; Rennie, P.; Sapunar, F.; Lowe, E.; Piccart, M., *J. Clin. Oncol.* **2008**, *26*, 1664-1670.
20. Robertson, J. F.; Lindemann, J.; Garnett, S.; Anderson, E.; Nicholson, R. I.; Kuter, I.; Gee, J. M., *Clin Breast Cancer* **2014**, *14*, 381-389.
21. de Ruijter, A. J.; van Gennip, A. H.; Caron, H. N.; Kemp, S.; van Kuilenburg, A. B., *Biochem. J.* **2003**, *370*, 737-749.
22. Kim, S. C.; Sprung, R.; Chen, Y.; Xu, Y.; Ball, H.; Pei, J.; Cheng, T.; Kho, Y.; Xiao, H.; Xiao, L.; Grishin, N. V.; White, M.; Yang, X. J.; Zhao, Y., *Mol Cell* **2006**, *23*, 607-618.
23. Struhl, K., *Genes Dev.* **1998**, *12*, 599-606.
24. Jovanovic, J.; Ronneberg, J. A.; Tost, J.; Kristensen, V., *Mol. Oncol.* **2010**, *4*, 242-254.
25. Paris, M.; Porcelloni, M.; Binaschi, M.; Fattori, D., *J. Med. Chem.* **2008**, *51*, 1505-1529.
26. Khan, O.; La Thangue, N. B., *Immunol. Cell. Biol.* **2012**, *90*, 85-94.
27. Haberland, M.; Montgomery, R. L.; Olson, E. N., *Nat. Rev. Genet.* **2009**, *10*, 32-42.
28. Mann, B. S.; Johnson, J. R.; He, K.; Sridhara, R.; Abraham, S.; Booth, B. P.; Verbois, L.; Morse, D. E.; Jee, J. M.; Pope, S.; Harapanhalli, R. S.; Dagher, R.; Farrell, A.; Justice, R.; Pazdur, R., *Clin. Cancer Res.* **2007**, *13*, 2318-2322.
29. Hodges-Gallagher, L.; Valentine, C. D.; Bader, S. E.; Kushner, P. J., *Breast Cancer Res. Treat.* **2007**, *105*, 297-309.
30. Restall, C.; Doherty, J.; Liu, H. B.; Genovese, R.; Paiman, L.; Byron, K. A.; Anderson, R. L.; Dear, A. E., *Int. J. Cancer* **2009**, *125*, 483-487.
31. Tu, Z.; Li, H.; Ma, Y.; Tang, B.; Tian, J.; Akers, W.; Achilefu, S.; Gu, Y., *Mol. Cell. Biochem.* **2012**, *366*, 111-122.
32. Fan, J.; Yin, W.-J.; Lu, J.-S.; Wang, L.; Wu, J.; Wu, F.-Y.; Di, G.-H.; Shen, Z.-Z.; Shao, Z.-M., *J. Cancer. Res. Clin. Oncol.* **2008**, *134*, 883-890.
33. Jang, E. R.; Lim, S.-J.; Lee, E. S.; Jeong, G.; Kim, T.-Y.; Bang, Y.-J.; Lee, J.-S., *Oncogene* **2004**, *23*, 1724-1736.
34. Munster, P. N.; Thurn, K. T.; Thomas, S.; Raha, P.; Lacevic, M.; Miller, A.; Melisko, M.; Ismail-Khan, R.; Rugo, H.; Moasser, M.; Minton, S. E., *Br. J. Cancer* **2011**, *104*, 1828-1835.
35. Mendoza-Sanchez, R.; Cotnoir-White, D.; Kulpa, J.; Jutras, I.; Pottel, J.; Moitessier, N.; Mader, S.; Gleason, J. L., *Bioorg. Med. Chem.* **2015**, *23*, 7597-7606.
36. Tang, C.; Li, C.; Zhang, S.; Hu, Z.; Wu, J.; Dong, C.; Huang, J.; Zhou, H.-B., *J. Med. Chem.* **2015**, *58*, 4550-4572.
37. Patel, H. K.; Siklos, M. I.; Abdelkarim, H.; Mendonca, E. L.; Vaidya, A.; Petukhov, P. A.; Thatcher, G. R. J., *ChemMedChem* **2014**, *9*, 602-613.
38. Gryder, B. E.; Rood, M. K.; Johnson, K. A.; Patil, V.; Raftery, E. D.; Yao, L.-P. D.; Rice, M.; Azizi, B.; Doyle, D.; Oyelere, A. K., *J. Med. Chem.* **2013**, *56*, 5782-5796.
39. Marinero, J. D. C.; Lapierre, M.; Cavailles, V.; Saint-Fort, R.; Vessieres, A.; Top, S.; Jaouen, G., *Dalton Trans.* **2013**, *42*, 15489-15501.
40. Pike, A. C.; Brzozowski, A. M.; Walton, J.; Hubbard, R. E.; Thorsell, A. G.; Li, Y. L.; Gustafsson, J. A.; Carlquist, M., *Structure (Camb)* **2001**, *9*, 145-153.
41. Tavera-Mendoza, L. E.; Quach, T. D.; Dabbas, B.; Hudon, J.; Liao, X.; Palijan, A.; Gleason, J. L.; White, J. H., *Proc. Nat. Acad. Sci.* **2008**, *105*, 8250-8255.
42. Lamblin, M.; Dabbas, B.; Spingarn, R.; Mendoza-Sanchez, R.; Wang, T.-T.; An, B.-S.; Huang, D. C.; Kremer, R.; White, J. H.; Gleason, J. L., *Bioorg. Med. Chem.* **2010**, *18*, 4119-4137.
43. Fischer, J.; Wang, T. T.; Kaldre, D.; Rochel, N.; Moras, D.; White, J. H.; Gleason, J. L., *Chem Biol* **2012**, *19*, 963-971.
44. Kaldre, D.; Wang, T. T.; Fischer, J.; White, J. H.; Gleason, J. L., *Bioorg. Med. Chem.* **2015**, *23*, 5035-5049.
45. One example of an HDACi unit in the core mimic a bridged bicyclic estrogen mimic has been reported. See Ref. 33.
46. Shiau, A. K.; Barstad, D.; Loria, P. M.; Cheng, L.; Kushner, P. J.; Agard, D. A.; Greene, G. L., *Cell* **1998**, *95*, 927-937.
47. Tanenbaum, D. M.; Wang, Y.; Williams, S. P.; Sigler, P. B., *Proc. Nat. Acad. Sci.* **1998**, *95*, 5998-6003.
48. Brzozowski, A. M.; Pike, A. C.; Dauter, Z.; Hubbard, R. E.; Bonn, T.; Engstrom, O.; Ohman, L.; Greene, G. L.; Gustafsson, J. A.; Carlquist, M., *Nature* **1997**, *389*, 753-758.
49. Dykstra, K. D.; Guo, L.; Birzin, E. T.; Chan, W.; Yang, Y. T.; Hayes, E. C.; DaSilva, C. A.; Pai, L.-Y.; Mosley, R. T.; Kraker, B.; Fitzgerald, P. M. D.; DiNinno, F.; Rohrer, S. P.; Schaeffer, J. M.; Hammond, M. L., *Bioorg. Med. Chem. Lett.* **2007**, *17*, 2322-2328.
50. Coe, P. L.; Scriven, C. E., *J. Chem. Soc. Perkin I* **1986**, 475-3.
51. Xue, F.; Zhao, J.; Hor, T. S. A.; Hayashi, T., *J. Am. Chem. Soc.* **2015**, *137*, 3189-3192.
52. Alkene **13** was also prone to isomerization, but only under more acidic conditions. The slightly increased stability of **13** may be due to the electron withdrawing pivaloyl group.

53. Bradner, J. E.; West, N.; Grachan, M. L.; Greenberg, E. F.; Haggarty, S. J.; Warnow, T.; Mazitschek, R., *Nat. Chem. Biol.* **2010**, 6, 238-243.
54. Alao, J. P.; Lam, E. W.; Ali, S.; Buluwela, L.; Bordogna, W.; Lockey, P.; Varshochi, R.; Stavropoulou, A. V.; Coombes, R. C.; Vigushin, D. M., *Clin. Cancer Res.* **2004**, 10, 8094-8104.
55. Reid, G.; Metivier, R.; Lin, C. Y.; Denger, S.; Ibberson, D.; Ivacevic, T.; Brand, H.; Benes, V.; Liu, E. T.; Gannon, F., *Oncogene* **2005**, 24, 4894-4907.
56. Yi, X.; Wei, W.; Wang, S. Y.; Du, Z. Y.; Xu, Y. J.; Yu, X. D., *Biochem Pharmacol* **2008**, 75, 1697-1705.
57. Prybylowski, P.; Obajimi, O.; Keen, J. C., *Breast Cancer Res. Treat.* **2008**, 111, 15-25.
58. Komorowsky, C.; Ocker, M.; Goppelt-Strube, M., *Journal of cellular and molecular medicine* **2009**, 13, 2353-2364.
59. Giandomenico, V.; Simonsson, M.; Gronroos, E.; Ericsson, J., *Mol. Cell. Biol.* **2003**, 23, 2587-2599.
60. Komatsu, N.; Kawamata, N.; Takeuchi, S.; Yin, D.; Chien, W.; Miller, C. W.; Koeffler, H. P., *Oncol Rep* **2006**, 15, 187-191.
61. Corbeil, C. R.; Englebienne, P.; Moitessier, N., *J Chem Inf Model* **2007**, 47, 435-449.
62. Pottel, J.; Therrien, E.; Gleason, J. L.; Moitessier, N., *J. Chem. Info. Model.* **2014**, 54, 254-265.
63. Fischer, J.; Wang, T.-T.; Kaldre, D.; Rochel, N.; Moras, D.; White, J. H.; Gleason, J. L., *Chem. Biol.* **2012**, 19, 963-971.
64. Lamblin, M.; Spingarn, R.; Wang, T.-T.; Burger, M. C.; Dabbas, B.; Moitessier, N.; White, J. H.; Gleason, J. L., *J. Med. Chem.* **2010**, 53, 7461-7465.
65. Hai, Y.; Christianson, D. W., *Nat. Chem. Biol.* **2016**, 12, 741-747.
66. Rink, S. M.; Yarema, K. J.; Solomon, M. S.; Paige, L. A.; Tadayoni-Rebek, B. M.; Essigmann, J. M.; Croy, R. G., *Proc. Nat. Acad. Sci.* **1996**, 93, 15063-15068.
67. Mitra, K.; Marquis, J. C.; Hillier, S. M.; Rye, P. T.; Zayas, B.; Lee, A. S.; Essigmann, J. M.; Croy, R. G., *J. Am. Chem. Soc.* **2002**, 124, 1862-1863.
68. Peng, K.-W.; Wang, H.; Qin, Z.; Wijewickrama, G. T.; Lu, M.; Wang, Z.; Bolton, J. L.; Thatcher, G. R. J., *ACS Chem. Biol.* **2009**, 4, 1039-1049.
69. Ciesielski, F.; Rochel, N.; Moras, D., *J. Steroid Biochem. Mol. Biol.* **2007**, 103, 235-242.
70. Zheng, L.; Wei, Q.; Zhou, B.; Yang, L.; Liu, Z. L., *Anticancer Drugs* **2007**, 18, 1039-1044.

8. Supplementary Material

BRET titration assay for **16**, antiproliferative data in ER-cells, primers for RT-PCR, details for synthesis of **18** and **29** and NMR Spectra.